

ABSORPTION OF LIGHT IN ANTIFERROMAGNETIC DIELECTRICS

V. V. EREMENKO and A. I. BELYAEVA

Physico-technical Institute of Low Temperatures, Ukrainian Academy of Sciences, Khar'kov

Usp. Fiz. Nauk 98, 27-70 (May, 1969)

1. Introduction

THE present review is devoted to questions of spectroscopy of magnetically-ordered crystals, which have been investigated in greatest detail theoretically and experimentally during the last 5-7 years. We shall deal primarily with antiferromagnetic dielectrics, the stoichiometric composition of which includes ions of the iron group (with unfilled 3d-shell) or of the rare-earth group (with unfilled 4f-shell).

The spectra of 3d and 4f ions introduced in the form of a small impurity in transparent diamagnetic crystals have been investigated in great detail. It was precisely the large number of spectrum investigations of such crystals that served as the scientific basis for the development of solid state lasers.

Recently, increasing attention has been paid to the study of the optical absorption spectra of crystals containing appreciable amounts of impurity 3d ions, when the light is absorbed not only by single ions but complexes of ions. The next step is to investigate magnetically-concentrated crystals, the stoichiometric composition of which includes magnetic ions with uncompensated magnetic moments of the unfilled 3d and 4f shells. Magnetically-concentrated crystals, when cooled below a definite temperature (Curie temperature T_C or Neel temperature T_N), go over into an ordered ferromagnetic or antiferromagnetic state. The features of the interaction of light with such crystals should be divided into two categories:

1. Features characteristic of both the magnetically ordered and the disordered (paramagnetic) state. These include questions connected with the splitting of terms in the crystal field, determination of the multiplicity and mechanism of the lifting of hindrances to optical transitions, the complication of the structure of the light absorption spectrum as a result of electron-phonon interaction, and the determination of the character of the electronic excitations—whether they are local or collective (excitons).

2. Light-absorption features connected with magnetic ordering of the crystals. These include first of all the changes of the electron spectrum under the influence of the exchange interaction, and also characteristic absorption-spectrum features due to electron-magnon interaction, change in the shape and width of the bands, the appearance of satellite bands in the optical spectrum, and the appearance of two-magnon and phonon-magnon bands in the infrared absorption spectrum.

Before we proceed to a consistent discussion of this problem, let us stop to discuss certain methodological details of the experimental study of light absorption in antiferromagnetic crystals.

2. Some Details of the Experimental Procedure

The greatest interest attaches to the study of light absorption in crystals that go over into the magnetically ordered state at low temperatures. In such cases the bands (or lines) of light absorption are sufficiently narrow to be able to observe subtle features of the spectrum: the shift and splitting of the absorption bands, the anomaly of the temperature dependence of their shape near the phase-transition temperature (T_C or T_N).

Apparatus for spectral investigations of magnetically ordered crystals must, above all, be equipped with cryostats having transparent windows, to permit measurements in a broad spectral and temperature range. There are many known constructions of such cryostats, the most successful among which are those developed by A. F. Prikhot'ko and co-workers.^[1] They are not intended, however, for magneto-optical investigations or for operation at temperatures below 4.2°K.

Figure 1 shows schematically the construction of a cryostat developed by V. N. Pavlov and V. V. Eremenko.^[2] The cryostat consists of four basic parts: a central tank 1 of capacity 850 cm³ with windows of special construction and an upper flange unit, a nitrogen

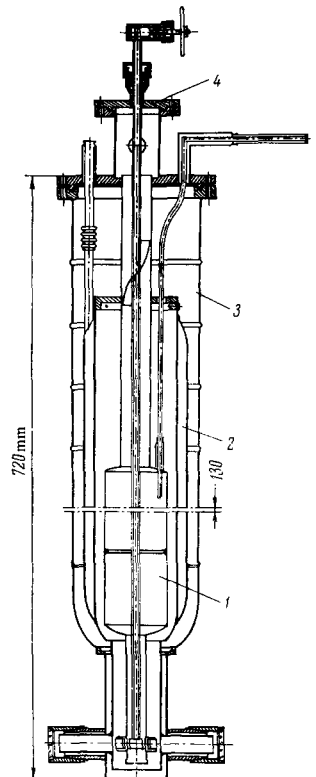


FIG. 1. Cryostat for magneto-optical investigations of crystals [2].

tank 2 with capacity 600 cm³, a vacuum jacket 3 with outside windows, and an upper removable flange 4 with movable rod and sample holder. The internal optical windows made of fused quartz are coaxially sealed in the lower narrowed-down portion of the tank. In spite of the very large difference in the thermal expansion coefficients of the metal and the quartz, the use of an adhesive composition based on ED-6 epoxy resin for vacuum sealing of the optical windows has made it possible to obtain windows that are free of the depolarizing effect. To decrease an appreciable fraction of the heat delivered to the liquid helium through the windows, tubular screens are used, which decrease greatly the solid angle in which the infrared thermal radiation propagates without obstruction. A high degree of blackness of the inner surface of the tube is obtained by cutting a thread strongly oxidizing its surface. A specially designed holder makes it possible to set the investigated crystal on the optical axis normally to the axis, and to rotate the crystal smoothly around this axis in its own plane so as to orient it correctly relative to the magnetic field and the polarizers. The cryostat makes it possible to operate at temperatures 1.3°K and below and retains the liquid helium (0.8 liters) for many hours (more than 24), a factor highly convenient for long exposures. The presence of a narrowed-down lower part makes it possible to carry out magneto-optical investigations using an SP-47g electromagnet in fields of intensity up to 30 kOe.

the procedure does not introduce noticeable errors. In the apparatus developed by V. V. Eremenko and Yu. A. Popkov^[4] (Fig. 2), short-duration (10⁻⁵ sec) powerful light pulses are obtained with the aid of gas-discharge xenon-filled tubes. The magnetic field and light pulses are synchronized with the aid of an electronic delay system, which makes it possible to apply to the flash lamp a discharge-triggering pulse at the instant when the magnetic field in the solenoid reaches maximum intensity. Since the single-crystal samples are quite small in size, solenoids producing magnetic fields of intensity up to 300 kOe can likewise have small dimensions. The latter circumstance makes it possible to immerse them directly into the cryogenic liquid, thus affording a large gain in the sense of increasing the magnetic field intensity, since cooling to low temperatures decreases the resistance of the winding material and accordingly decreases greatly the loss of the energy stored in the battery to Joule heat. Although cooling decreases also the specific heat of the solenoid winding material (copper or aluminum), the maximum ratio c_v/ρ (c_v—specific heat, ρ—electric resistivity) for the aforementioned metals lies near the boiling temperature of liquid hydrogen.^[7]

In the case of pulsed magneto-optical investigations, however, it must be remembered that the relaxation processes can strongly influence the results. In the cited reference, special control was exercised by vary-

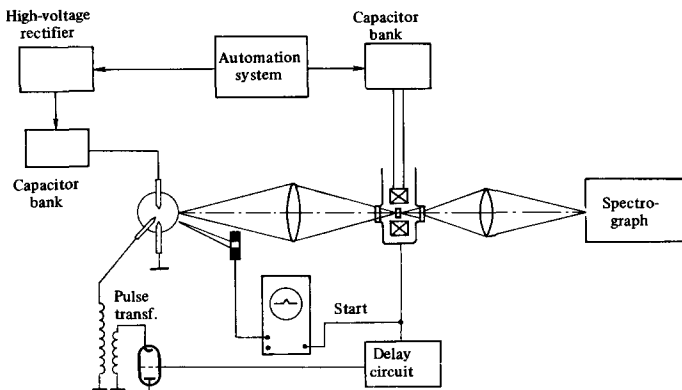


FIG. 2. Setup for magneto-optical investigations in pulsed magnetic fields [4].

The fields that can be obtained with the aid of ordinary electromagnets are insufficient for the study of antiferromagnets with appreciable magnetic crystallographic anisotropy. In this case the magnetic structure of the crystal can be changed only in a magnetic field whose intensity approaches the intensity of the internal effective magnetic fields (10⁵ Oe and higher). In spite of progress in the technique of superconducting solenoids, the strongest magnetic fields are obtainable so far with the aid of a pulsed technique—most frequently by discharging a powerful capacitor bank through a solenoid cooled with liquid-hydrogen or helium. Recently reported devices for magneto-optical investigations of crystals in pulsed magnetic fields^[3-5] make use of an idea of P. L. Kapitza, whereby the investigated spectrum is photographed by short flashes synchronized with the pulses of the magnetic field.^[6] If the duration of the light flash is much shorter than the duration of the magnetic-field pulse, then the pulse character of

ing the magnetic-field pulse duration. Since no influence of the duration of the magnetic pulse has been noted, it must be assumed that the results correspond in practice to a stationary magnetic field. The pulse procedure can nevertheless be used to measure the spin-lattice relaxation time if this time is large, on the order of 10⁻³ sec.^[4,5]

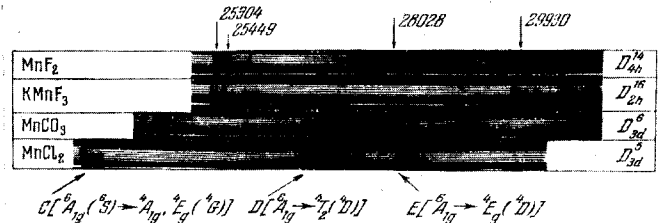


FIG. 3. Absorption spectra of crystals whose stoichiometric composition includes Mn²⁺ ions (T = 20.4°K).

To observe the fine details of the light-absorption spectrum in magnetically ordered crystals, it is necessary to use instruments with high resolution, such as DFS-13 diffraction spectrograph (with linear dispersion 2 Å/mm) in the visible and ultraviolet regions of the spectrum, and two-beam spectrophotometers (for example, IKS-22) in the infrared region. In the latter case, however, it was necessary to modify the instrument somewhat in order to make it suitable for the study of small samples. Most foreign investigations in the visible region of the spectrum were performed with diffraction spectrographs having a linear dispersion 2.5 Å/mm.

I. LIGHT ABSORPTION BY MAGNETICALLY-CONCENTRATED CRYSTALS IN THE PARAMAGNETIC STATE

In this chapter we confine ourselves to crystals containing iron-group ions in their stoichiometric composition. Most antiferromagnets belong precisely to this group of substances. Absorption of light by such crystals is due to the optical transitions between levels of the unfilled 3d-shell of the magnetic ions, as is evidenced primarily by the similarity between the spectra of substances whose stoichiometric composition includes different ligands (nonmagnetic ions), but the same ion with unfilled 3d-shell. This circumstance is illustrated in Fig. 3, using as an example a number of substances containing Mn^{2+} ions and having different crystallographic structures. The general similarity of the spectrum is obvious, and differences are noted only in details of their structure.

3. Structure of Spectrum. Applicability of Crystal-field Theory. Electron-phonon Interaction

To identify the absorption spectrum of a magnetically-concentrated crystal, it is customary to use the theory of the crystal field. In this theory it is assumed that the paramagnetic ion is surrounded in the crystal by cation charges producing the "intracrystalline field." In this case the problem reduces to an analysis of the Stark effect in an electric field of given intensity and symmetry. Since for iron-group ions the energy of interaction with the crystal field is smaller by two orders of magnitude than the energy of the Coulomb interaction inside the ion, the influence of the crystal field on the energy levels of the ions is calculated by perturbation theory. The main premises of the crystal-field theory were formulated by Bethe.^[8] The results of his investigation were subsequently developed and applied to the calculation of optical spectra and electron paramagnetic resonance spectra of the 3d ions Mn^{2+} , Co^{2+} , Ni^{2+} , Fe^{2+} in crystals, and have been explained in sufficient detail in monographs and in reviews.^[9,10] We shall therefore not dwell on this theory in detail.

To demonstrate the applicability of the theory of the crystal field to the explanation of the spectra of magnetically-concentrated crystals, let us consider the simplest case, the absorption of the CoF_2 crystal in the near infrared. This absorption is due to optical transitions between the components of the principal term of the Co^{2+} ion, namely ${}^4F_{9/2}$, split in the field of the crystal, making its interpretation much simpler in

comparison with the absorption in the region of shorter wavelengths, due to transitions between different terms.

Cobalt fluoride has the structure of rutile (space group D_{2h}^{14}).^[11] The Co^{2+} ion is surrounded by six fluorine ions F^- , which are practically equidistant from it. Therefore, although the actual symmetry of the field at the location of the Co^{2+} is orthorhombic, D_{2h} , it can be regarded as cubic in first approximation. This fact predetermines the calculation scheme. We consider first the splitting in a field of predominantly cubic symmetry. As the weaker perturbations we take into account the true, rhombic symmetry of the Co^{2+} site and the spin-orbit interaction. The procedure of such calculations was described in detail in the monographs of Balhausen^[9] and Griffiths.^[12]

In a crystal field of cubic symmetry, the principal term of the cobalt ion ${}^4F_{9/2}$ is split into three components, ${}^4A_{2g}$, ${}^4T_{1g}$, and ${}^4T_{2g}$,* i.e., into an orbital singlet and two orbital triplets. The splitting of the ${}^4F_{9/2}$ term with allowance for the orthorhombic component of the crystal field and the spin-orbit interaction was calculated by Kamimura and Tanabe^[13] and by A. I. Zvygin.^[14] In the latter case, the results were presented in the form of plots of the energies of the split levels against parameters of the spin-orbit interaction (λ), and of the crystal field of axial (trigonal) and rhombic symmetry (Δ and Γ). The best agreement with experiment is obtained at the following values of the parameters: $\lambda = -157 \text{ cm}^{-1}$, $\Delta = -707 \text{ cm}^{-1}$, and $\Gamma = -183 \text{ cm}^{-1}$. However, such an analysis does not make it possible to identify completely all the details of the fine structure of the CoF_2 absorption spectra. For example, 11 bands in the antiferromagnetic state and not less than seven in the paramagnetic state ($T > T_N$) were observed experimentally in the CoF_2 spectrum in the frequency region $800\text{--}2000 \text{ cm}^{-1}$.^[15,16] On the other hand, the presented calculation scheme makes it possible to explain the presence of only five absorption bands in this frequency region.

A more rigorous calculation of the principal term ${}^4F_{9/2}$ in CoF_2 was made by V. I. Peresada and E. S. Syrkin^[17] for the case when the deviation from cubic symmetry is large and the influence of the low-symmetry field cannot be regarded as a small correction to the interaction between the electrons and the cubic-symmetry field. They considered not only the first coordination sphere of the neighboring F^- ions, but also a large number of succeeding spheres. The need for this follows from the following considerations: the second coordination sphere consists of Co^{2+} ions whose charge (2e) is double that of the F^- ions. The number of cobalt ions closest to the chosen one is eight and that of fluorine ions is six, while the distances between the considered ions and the neighbors are commensurate ($Co^{2+}\text{--}Co^{2+} = 3.3 \text{ \AA}$ and $Co^{2+}\text{--}F^- = 2.4 \text{ \AA}$). The calculation of Peresada and Syrkin can explain the appearance of a large number of absorption bands in the frequency region $800\text{--}2000 \text{ cm}^{-1}$ when account is taken of the additional exchange splitting (lifting of the Kramers degeneracy). On the other hand, "extra" bands are observed

*We use throughout Millikan's notation for the irreducible representations.

experimentally in this spectral region at temperatures greatly exceeding the Neel temperature T_N . In addition, calculation predicts the appearance in the CoF_2 spectrum of two absorption bands in the regions ~ 6000 and ~ 4000 cm^{-1} , whereas experimentally only one band is observed with $\nu_{\text{max}} = 7140$ cm^{-1} .

It must thus be admitted that none of the calculation schemes agrees fully with experiment even in the case of the Co^{2+} and CoF_2 infrared spectrum due to transitions between the components of the splitting of the one term ${}^4F_{9/2}$. Therefore, in the case of the optical and ultraviolet spectra, when transitions between different terms must be considered, there are hardly any grounds at all for such a detailed comparison with a calculation that takes into account the deviation of the field symmetry from cubic.

The theory of the crystal field in the case of magnetically-concentrated crystals has, as a rule, a limited application and can explain only the common features of the spectrum. On the other hand, for an analysis of its fine structure it is necessary to resort to mechanisms that are peculiar to magnetically-concentrated crystals and to the magnetically-ordered state. For example, the "extra" bands in the $800\text{--}2000$ cm^{-1} region of the CoF_2 spectrum can be explained^[13] by assuming that when the infrared radiation is absorbed there are realized double optical transitions in CoF_2 : one photon excites simultaneously two ions that are coupled by exchange interaction. Then, combining the energy intervals between the components of the split level ${}^4T_{1g}({}^4F_{9/2})$,* it is possible to explain all the infrared absorption bands of CoF_2 (Fig. 4). Such "double" transitions acquire a noticeable intensity only when the interaction between the ions is appreciable, and, of course, are peculiar to magnetically-concentrated crystals. To explain the fine structure of the spectrum in the region of the ${}^4T_{1g} \rightarrow {}^4T_{2g}$ and ${}^4T_{1g} \rightarrow {}^4A_{2g}$ transitions between the components of the splitting of the ground state ${}^4F_{9/2}$ in CoF_2 , Van der Ziel and Guggenheim^[18] make use of effects connected with collective excitation of the spin system in the crystal. Similar complications of the fine structure of the spectrum, connected with singularities of the magnetically ordered state, were observed in many other compounds containing Mn^{2+} and Ni^{2+} ions, and will be discussed in Ch. II of the review.

The structure of the optical spectra of magnetically ordered crystals may become complicated as a result of the electron-phonon interaction. The light-absorption spectra of these crystals may reveal electron-vibrational bands forming equidistant series. Figure 5 shows by way of an example the electron-vibrational structure in the absorption spectrum of MnCl_2 crystals, which was investigated in detail a number of times. This is a typical example of a discrete structure consisting of narrow absorption bands whose frequencies can be described by serial relationships of the type

$$\nu_n = \nu_0 + n_k \nu_k,$$

where ν_n is the frequency of the n-th term of the series,

*Here, as usual, we employ the following notation for the levels of an ion in a field of cubic symmetry: the irreducible representation of the O_h group is indicated, and the state of the free ion, from which the considered state of the ion in the crystal originated, is shown in the parentheses.

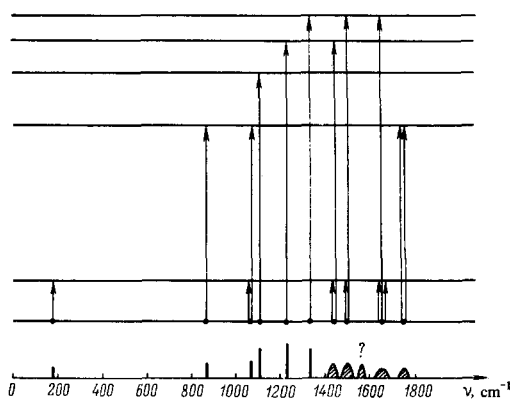


FIG. 4. Scheme of single and double transitions, explaining the structure of the absorption spectrum of CoF_2 in the infrared region.

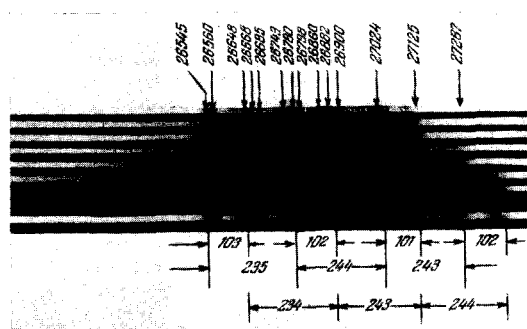


FIG. 5. Electron-vibrational structure of the ${}^6A_{1g}({}^6S) \rightarrow {}^4T_{2g}({}^4D)$ transition in the absorption spectrum of MnCl_2 ($T = 20.4^\circ\text{K}$).

ν_0 is the frequency of the purely electronic line, n is an integer, and ν_k is the limiting frequency of the k -th branch. Such series are frequently observed in optical absorption and luminescence spectra of molecular crystals and of crystals containing impurities and local centers. They are typical of the case of weak electron-phonon interactions. It is not surprising that a weak coupling is realized also for the crystals considered by us, with partially screened 3d shell. The absorption spectra of MnCl_2 (see Fig. 5) obtained at 20.4°K , is very distinct and makes the electron-vibrational analysis very convincing. The interval $\Delta\nu \sim 240$ cm^{-1} , with the aid of which the electron-vibrational series are constructed, is reliably separated. Its magnitude is close to the lattice-vibration frequency determined from the absorption in the infrared region: $\nu_{\text{vib}} \sim 220$ cm^{-1} .^[19] MnCl_2 is not the only example of magnetically-concentrated crystals with electron-vibrational structure of the optical spectrum. An equidistant structure, for example, was observed in the absorption spectra of CoCO_3 and NiF_2 .^[20] Figure 6 shows the spectrum in the region of the ${}^3A_2 \rightarrow {}^1T_2$ transition of NiF_2 ^[21] and $T = 20.4^\circ\text{K}$. It also shows the frequency intervals between the absorption lines, which are very close in magnitude to the vibrational frequencies of the NiF_2 lattice measured directly in the infrared region of the spectrum.^[22] The optical phonons undoubtedly take part in the formation of the absorption bands of fluorides of transition metals with perovskite structure, as shown convincingly by Balkanski and co-authors^[23] with KNiF_3 as an example. Thus, the interaction with the lattice vibration is an im-

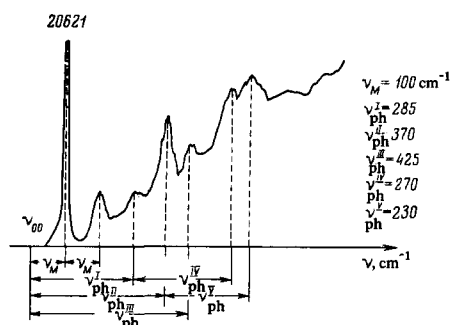


FIG. 6. Structure of the absorption spectrum of NiF_2 in the region of the ${}^3A_2 \rightarrow {}^1T_2$ transition ($T = 20.4^\circ\text{K}$) [21].

portant factor in the formation of the fine structure of the absorption spectrum of magnetically-concentrated crystals.

4. Multiplicity and Mechanisms of Allowing Forbidden Optical Transitions in Crystals

The multiplicity of optical transitions is usually determined experimentally with the aid of polarization investigations. This method is based on simple considerations: if the transition is electric-dipole, then the intensity of the corresponding absorption band should be determined by the orientation of the electric vector of the light wave \mathbf{E}_ω relative to the axes of the anisotropic crystal; on the other hand, in the case of a magnetic dipole transition, the decisive factor is the orientation of the magnetic field of the light wave \mathbf{H}_ω . The absorption anisotropy was investigated in greatest detail using tetragonal fluorides CoF_2 [16] and MnF_2 [24] as examples.

Figure 7 illustrates by way of an example the absorption anisotropy in the region of the ${}^6A_{1g}({}^6S) \rightarrow {}^4A_{1g} \rightarrow {}^4E_g({}^4G)$ transition in the MnF_2 spectrum. We see that the intensity of the bands is determined by the orientation of the vector \mathbf{E}_ω relative to the tetragonal C_4 axis and does not depend on the orientation of \mathbf{H}_ω or on the direction of propagation of light. Similar investigations show that all the absorption bands having an appreciable intensity in spectra of magnetically-concentrated crystals are due to electric-dipole transitions. On the long-wave side, they frequently are accompanied by weak and very narrow lines of magnetic dipole origin, the intensity anisotropy of which is determined by the orientation of the magnetic vector \mathbf{H}_ω of the light wave.

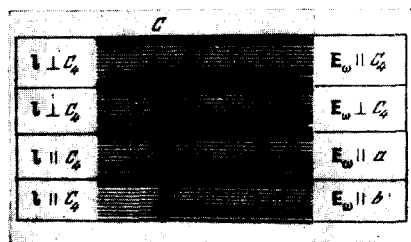


FIG. 7. Dichroism of absorption in the region of the C-group of bands (see ${}^6A_{1g}({}^6S) \rightarrow {}^4A_{1g} \rightarrow {}^4E_g({}^4G)$ transition) in the spectrum of MnF_2 ($T = 28.4^\circ\text{K}$) [24]. I - incident-light vector; \mathbf{E}_ω - electric vector of light wave; C_4 - tetragonal crystal axis, a and b - twofold axes perpendicular to C_4 .

The conclusion that most absorption bands have a dipole character is far from trivial. Indeed, the transitions under consideration, within the limits of the 3d shell, are parity forbidden (the Laporte rule [25]) and most frequently spin forbidden (for example, all the transitions in the 3d shell of the Mn^{2+} ion). At the same time, the intensities of the observed bands are sufficiently large. The oscillator strengths* of the absorption bands (10^{-8} - 10^{-5}) are frequently noticeably larger than in the case of magnetic dipole transitions. Apparently, both hindrances are lifted to some degree in the crystal.

The question of the lifting of the parity forbiddenness was considered in detail by Van Vleck. [26] This forbiddenness may be violated if a mixing of the orbital states with different parities takes place. Such a mixing can be induced in the crystal if the crystal field has no symmetry center, or else when the ion is displaced from the symmetry center as a result of its interaction with non-symmetrical oscillations of the surrounding ions.

Most magnetically-concentrated crystals have symmetry centers. In addition, for the observed transitions, the initial and final levels of the ion in the crystal are even. Therefore only the second mechanism of allowing the optical transitions is possible, as shown in Fig. 8. The oscillations of the crystal lattice displace the paramagnetic ion away from the symmetry center, mixing thereby the states of both parities.

By way of an example of an experimentally observed manifestation of the Van Vleck mechanism let us consider the behavior of the absorption band with a maximum frequency $\nu_{\text{max}} \approx 7140 \text{ cm}^{-1}$, observed in the near infrared region of the spectrum for all cobalt compounds, and identified with a transition between the components of the splitting of the principal term ${}^4F_{9/2}$ in a field of O_h symmetry: ${}^4T_{1g} \rightarrow {}^4T_{2g}$. A group-theoretical analysis of the oscillations of the nearest neighbors of the Co^{2+} ion shows that they include modes such that the interaction with them allows the ${}^4T_{1g} \rightarrow {}^4T_{2g}$ transition. According to the theory, [27] the intensity of the electric dipole transitions that are allowed as a result of interaction with phonons is stronger by approximately two orders of magnitude than the allowed magnetic dipole or electric quadrupole transitions and is weaker by approximately three orders of magnitude than the allowed electric dipole transitions. The experimentally measured intensity of the ${}^4T_{1g} \rightarrow {}^4T_{2g}$ transition in CoF_2 agrees with these estimates.

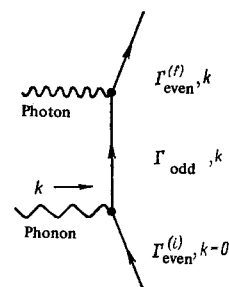


FIG. 8. Van Vleck mechanism of allowing the electric-dipole transitions in crystals with symmetry centers [26].

*We are speaking here of the oscillator strengths of the individual absorption bands, and not of the entire group pertaining to a definite transition.

In the Van Vleck mechanism of allowing the optical transition, the integral intensity of the absorption band should depend strongly on the temperature. An approximate analysis made by Liehr and Ballhausen^[27] shows that this dependence can be described by the expression

$$J \sim \text{cth} \left(\frac{h\nu_k}{2kT} \right), \quad (4.1)$$

where $h\nu_k$ is the energy of the phonon, the interaction with which allows the transition. The temperature dependence of the integral intensity^[28] of the ${}^4T_{1g} \rightarrow {}^4T_{2g}$ transition in the CoF_2 spectrum is well described by expression (4.1) with $h\nu_k \approx 0.056$ eV (450 cm^{-1}). This band has a similar behavior in the spectrum of other cobalt compounds. The values of the vibrational frequencies of CoCO_3 (0.054 eV), CoO (0.070 eV), and CoCl_2 (0.030 eV) were determined from data on the temperature dependence of the integral intensity of the band of the ${}^4F_{1g} \rightarrow {}^4T_{2g}$ transition.^[16,29] The values of the vibrational frequencies are close to those obtained independently by investigating the vibrational spectrum of these crystals in the infrared region. It should be noted that the limiting frequencies of the phonon branches obtained from the temperature dependence of the intensity of the ${}^4T_{1g} \rightarrow {}^4T_{2g}$ band are close for the crystals CoO , CoF_2 , and CoCO_3 , and differ from the frequency for CoCl_2 . On the other hand, the frequency $\nu_k \approx 220 \text{ cm}^{-1}$ for CoCl_2 is typical of chlorides with a layered structure, and was recently obtained for CoCl_2 directly in the vibrational spectrum, from the absorption in the infrared region.^[30] This fact confirms once more the electron-phonon mechanism of formation of this absorption band.

It can thus be stated that the hypothesis of the electron-phonon mechanism of allowing the optical transitions within the 3d shell of ions contained in crystals having an inversion center is confirmed, with the ${}^4T_{1g} \rightarrow {}^4T_{2g}$ transition in the spectrum of cobalt compounds as the example.

Of importance in the lifting of the spin forbiddenness is the exchange interaction between magnetic ions. Even in the case of crystals containing small amounts of such ions, this interaction leads to the formation of exchange-coupled ion pairs.^[31-34] The exchange-interaction operator of the pair of ions is of the form

$$\hat{V}_{S_1 S_2} = A \hat{S}_1 \hat{S}_2, \quad (4.2)$$

where A is the exchange-interaction constant (the exchange integral) and \hat{S}_1 and \hat{S}_2 are the spin operators of the first and second ion, respectively. The eigenvalues of the operator (4.2) are

$$V_{S_1 S_2} = A S_1 S_2 = \frac{A}{2} [S(S+1) - S_1(S_1+1) - S_2(S_2+1)] \quad (4.3)$$

(S —eigenvalue of the total spin momentum of the exchange-coupled ion pair). If we are interested in the relative positions of the levels, then the splitting energy can be written in the form

$$\frac{1}{2} A S(S+1). \quad (4.4)$$

The exchange-interaction constant A is positive in the case of ferromagnetic coupling in the pair, and negative if the coupling is antiferromagnetic. When $A > 0$, the lowest of the splitting components is the state with the minimum possible S , i.e., $S = |S_1 - S_2|$; if $A < 0$, the

lowest state is the one with $S = S_1 + S_2$. Let us consider by way of an example the most investigated case of an exchange-coupled pair of manganese ions. In the ground state $S_1 = S_2 = 5/2$, and in the excited state $S_1 = 5/2$ and $S_2 = 3/2$, i.e., only one Mn^{2+} ion in the pair is excited when light is absorbed. In such a case it is easy to obtain with the aid of (4.3) the spectrum of the pair, by starting from the spectrum of the free ion. Four absorption lines are then obtained, corresponding to the selection rule $\Delta S = 0$,^[31,32] which are much more intense than the forbidden single-ion transitions, for which $\Delta S_1 \neq 0$. This is precisely why the pair absorption could be observed in a cubic ZnS crystal with small admixture of manganese (1–2%).^[31] The concentration dependence of the pair absorption of light should be unusual, since the number of pairs depends nonlinearly on the concentration of the absorbing ions (violation of Beer's law).

In magnetically-concentrated crystals, which are compounds of transition-metal ions with nonmagnetic ions, the exchange interaction should have a particularly strong effect on the intensity of the optical absorption bands. The analysis can be reduced to the one described above by representing the exchange interaction of the magnetic ions as a superposition of pair interactions. In any case, the experimentally observed violation of Beer's law in many solid solutions, $\text{KMnF}_2\text{--KZnF}_3$,^[32] $\text{KMnF}_3\text{--KNiF}_3$,^[35,36] and $\text{KMnF}_3\text{--KCoF}_3$,^[35] and the anomalously large intensities of the absorption bands in the spectra of the pure crystals KMnF_3 and RbMnF_3 ^[37] apparently offer unambiguous evidence that an appreciable role is played by exchange interaction in the lifting of the spin forbiddenness.

The examples considered in this section show that electron-phonon interaction is frequently important in the lifting of the parity forbiddenness, while the spin forbiddenness can be lifted as a result of exchange interaction. These two mechanisms, however, are not universal. One can cite a number of examples in which the band intensity is independent of the temperature, yet Beer's law holds (for example, the D group of bands in MnF_2). In these cases, the considered mechanisms are of low effectiveness, and the decisive role is played by other mechanisms, not yet explained. Worthy of attention, in particular, is the mechanism of excitation of transitions with a change of spin as a result of spin-orbit interaction.^[38]

5. Band Shape and Exciton Character of Light Absorption

So far we have tacitly assumed that the absorption of light by the transition-group ions in crystals is analogous to the absorption by local centers. In the preceding section, to be sure, we already mentioned the important role of "pair" effects in crystals, even those with small concentrations of 3d ions. In the limiting case, however, that of magnetically concentrated crystals, one cannot speak of single ions or of pairs. Ions with unfilled 3d shells are arranged in the crystal strictly periodically. In this connection, one can state a priori that the electron excitation due to the photon absorption, not being localized within a single unit cell, will migrate over the crystal. This leads to a collective excitation of the crystal or to the formation of an exciton wave.

In the case of magnetically-concentrated crystals

with 3d or 4f ions, when the coupling inside the ion is stronger than between ions and the radius of the electronic excitation is limited by the unfilled shell, one should speak of generation of Frenkel excitons rather than Wannier-Mott excitons. In this sense, the singularities peculiar to molecular crystals may appear in the spectra of the crystals under consideration. On the other hand, a detailed investigation of molecular crystals has made it possible to formulate the basic criteria of exciton absorption, among which one must include first of all the Davydov splitting into polarized bands, the number of which is determined by the number of non-equivalent molecules (ions) in the unit cell, and the details of the absorption-band shape. The Davydov splitting of light-absorption bands in an anisotropic magnetically concentrated crystal, using the ${}^4H_2 \rightarrow {}^2E$ transition in Cr_2O_3 as an example, was recently observed by Van der Ziel.^[39] In the absence of an external magnetic field, only one component of the Davydov doublet is observed experimentally, while the other appears in an external magnetic field parallel to the C_3 axis of the crystal. This result could be understood within the framework of the exciton theory. The interpretation of the observed transitions, based on this theory, is shown in Fig. 9. The Davydov splitting between the levels A_1 and A_2 can actually not be observed in a zero external field, since, by virtue of the selection rules, the excitation of the A_1 exciton is possible only in an external magnetic field parallel to the C_3 axis of the crystal.^[39] Extrapolation to a zero field yields for the Davydov splitting a value equal to 3.75 cm^{-1} , which is expressed in terms of the diagonal terms of the Hamiltonian of the magnetic interaction between the A_1 and A_2 excitons.

A splitting of the same order was observed for the $\nu = 25143.5 \text{ cm}^{-1}$ line in cubic antiferromagnet RbMnF_3 .^[40] The antiferromagnet RbMnF_3 , owing to the cubic structure, has a small anisotropy field, making it possible to vary smoothly, by means of a relatively weak external magnetic field ($H \sim 3\text{--}5 \text{ kOe}$), the direction of the magnetic moments of its sublattices. The measurements were made on the line ν , whose half-width did not exceed 2 cm^{-1} . The line ν split into a doublet when the external field orientation was along the fourfold [100] and threefold [111] axes and did not react to application of an external field of intensity up to 25 kOe along the [110] axis (Fig. 10). Accordingly, the angular dependences of the splitting of the line ν are in the form of the rosettes shown in Fig. 11. In a strong magnetic field ($H \sim 200 \text{ kOe}$), the splitting anisotropy has qualitatively a different character: doublet splitting is observed at $H \parallel [110]$, and its magnitude increases with increasing field intensity, while at other orientations of H the splitting decreases at such a high field intensity (Fig. 12).

The results of the investigation of the anisotropy of the observed effect were analyzed by using the data of Cole and Ince^[41] concerning the change of the magnetic structure of RbMnF_3 as a function of the orientation and intensity of external magnetic field. Below the temperature $T_N = 82^\circ\text{K}$, RbMnF_3 becomes antiferromagnetic with an easy-magnetization axis parallel to the diagonal of the cube [111]. When the intensity of the external magnetic field $H \parallel [100]$ is increased, the magnetic

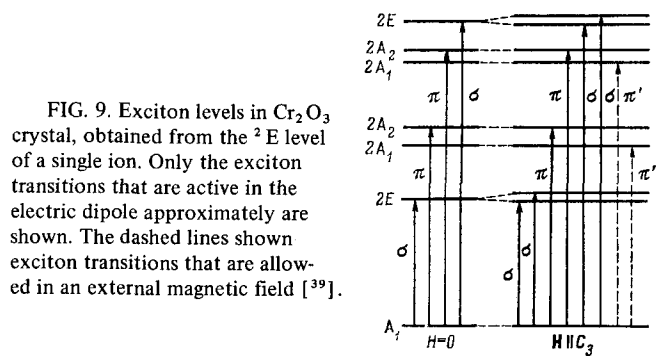


FIG. 9. Exciton levels in Cr_2O_3 crystal, obtained from the 2E level of a single ion. Only the exciton transitions that are active in the electric dipole approximately are shown. The dashed lines shown exciton transitions that are allowed in an external magnetic field^[39].

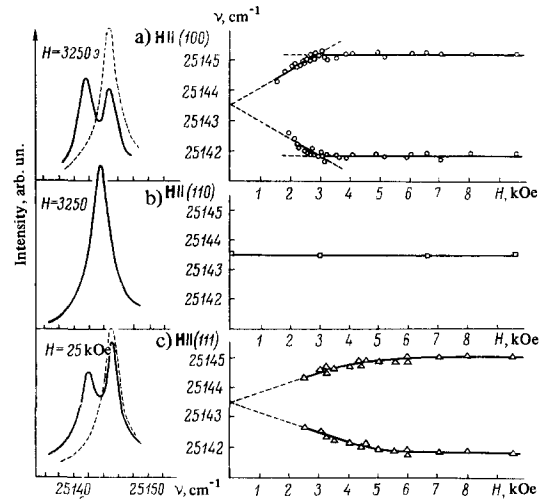


FIG. 10. Zeeman splitting of the 25143 cm^{-1} line in the spectrum of the cubic and antiferromagnet RbMnF_3 ($T = 4.2^\circ\text{K}$)^[40]. Dashed curve — $E_\omega \perp H$, $H_\omega \perp M_j$; solid curve — $E_\omega \parallel H$, $H_\omega \perp H$.

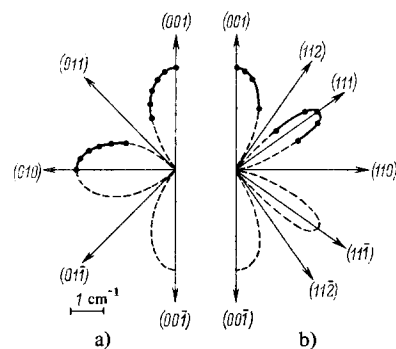


FIG. 11. Anisotropy of splitting of the 25143 cm^{-1} line in the RbMnF_3 spectrum ($T = 4.2^\circ\text{K}$, $H = 5 \text{ kOe}$)^[40]. a) H in (100) plane, b) H in (110) plane.

moments rotate smoothly away from the [111] axis, and become perpendicular to the field along the two-fold axis [110] when $H > H_c = \sqrt{1.5}H_A H_E$. When $H \parallel [110]$, no change in the magnetic symmetry of the crystal takes place in fields of low intensity $H \ll H_E$. The case $H \parallel [111]$ is interesting. Special investigations have shown that in a field $H = \sqrt{2}H_A H_E$ there is no turning over of the magnetic sublattices. Apparently, even in small fields, the magnetic moments become

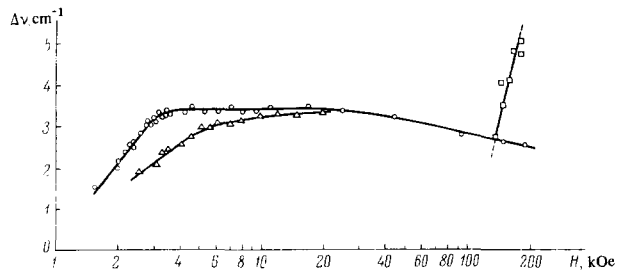


FIG. 12. Dependence of the splitting of the 25143 cm^{-1} line on the external-field intensity ($T = 4.2^\circ \text{K}$) [40]. $\circ - \mathbf{H} \parallel (100)$; $\Delta - \mathbf{H} \parallel (111)$; $\square - \mathbf{H} \parallel (110)$.

aligned along one of the three other threefold axes at an angle 70° to the field. With increasing field, they rotate and become perpendicular to the field only in a sufficiently strong field.

In fields $H \gg H_c$ ($H \sim 2 \times 10^5 \text{ Oe}$), "tilting" of the magnetic sublattices occur and a moment appears along the external field. The "tilt" angle ($t \sim H/2H_E$) does not exceed 10° in fields up to 200 kOe. Thus, the observed anisotropy of the splitting of the $\nu = 25143.5 \text{ cm}^{-1}$ band in RbMnF_3 is determined uniquely by the orientation of the magnetic moments \mathbf{M}_i of the sublattices relative to the crystallographic axis.

A group-theoretical analysis with allowance for the effective magnetic field of the exchange interaction shows that complete lifting of the degeneracy for all the excited levels of the Mn^{2+} ion. However, the spatial degeneracy, which remains in a crystal with two Mn^{2+} ions in a magnetic unit cell can be lifted only as a result of resonant interaction (Davydov splitting). The splitting of the ν band in RbMnF_3 is observed only at a definite direction of the magnetic moment \mathbf{M}_i of the crystal, namely along the $[110]$ axis, thus showing that the Davydov splitting has a sharp anisotropy.

An analysis of the band shape does not permit a unique determination of the character of the optical transitions. Of course, the dispersion of the energy in the exciton band $\epsilon = \epsilon(\mathbf{k})$ affects the shape of the exciton absorption bands and its temperature dependence, but it is impossible to establish quantitative differences for the local and exciton transitions. The mechanism of formation of the absorption-band contour for local centers or "localized" excitons (i.e., with a narrow band) was investigated theoretically in sufficient detail. [42-44] Two cases are possible here—of weak and strong electron-phonon coupling. In the former case the band shape due to the single-phonon processes is close to a Lorentz shape. On the other hand, in the case of a strong electron-phonon interaction, multiphonon transitions occur and the band shape is Gaussian. For comparison with experiment, we can use the approximate expressions for the Gaussian curve

$$f(x) = \frac{1}{\beta \sqrt{\pi}} \exp \left\{ - \left(\frac{x}{\beta} \right)^2 \right\}, \quad (5.1)$$

which was tabulated by Elste, [45] or for a Lorentz curve

$$K(\nu) \sim \frac{\frac{\delta}{2} + 2\alpha(\nu - \nu_0)}{(\nu - \nu_0)^2 + \left(\frac{\delta}{2} \right)^2}; \quad (5.2)$$

here $K(\nu)$ is the dimensionless absorption coefficient,

ν_0 the frequency of the optical transition, ν the running frequency, δ the half-width of the band, and α its asymmetry

$$\alpha = \frac{(\nu_{+1/2} - \nu_0) - (\nu_0 - \nu_{-1/2})}{\delta/2}, \quad (5.3)$$

$\nu_{\pm 1/2}$ are the frequencies at which $K = 0.5K_{\text{max}}$ on the short-wave (+) and long-wave (-) sides. A more consistent formula, however, is the one proposed by Rashba, which takes into account the linear term in the expansion of the damping factors $\gamma(\omega)$ not only in the numerator but also in the denominator. [43]

$$K(\nu) \sim \frac{\frac{\delta}{2} + 2\alpha(\nu - \nu_0)}{(\nu - \nu_0)^2 + 2\delta\alpha(\nu - \nu_0) + \left(\frac{\delta}{2} \right)^2}. \quad (5.4)$$

A few words must be said concerning the asymmetry of the exciton bands. It depends strongly on the structure of the exciton band. If states close to the top of the exciton band (where the effective mass $m^* < 0$) take part in the optical transition, then the absorption band has a more developed long-wave wing, i.e., negative asymmetry α . On the other hand, if $m^* > 0$, then $\alpha > 0$.

The experimental shape of the narrow absorption bands was investigated in detail using as an example magnetically concentrated crystals—fluorides and carbonates of manganese and cobalt. [24, 46-49] Most narrow light-absorption bands in these crystals have a Lorentz shape, at low temperatures, and in some bands there is observed a clearly pronounced "red" asymmetry, for example the D_1 band in the spectrum of MnF_2 (Fig. 13). These facts do not contradict the statement that excitons are produced in magnetically concentrated crystals when light is absorbed. However, investigations of the spectra of these crystals yield no unique proof of the appearance of exciton effects, neither in the structure of the spectra nor in the band shape. On this basis, it was proposed that the band widths of the Frenkel excitons connected with the excitation of the 3d shell of transition ions contained in the investigated crystals are sufficiently small, and that their effective masses are large.

A more unique proof of the exciton nature of the light-absorption bands in magnetically concentrated crystals was obtained in an experimental study of the Zeeman effect in antiferromagnetic crystals; these will be discussed somewhat later (Sec. 7). On the other hand, measurements of the frequencies of the combined elec-

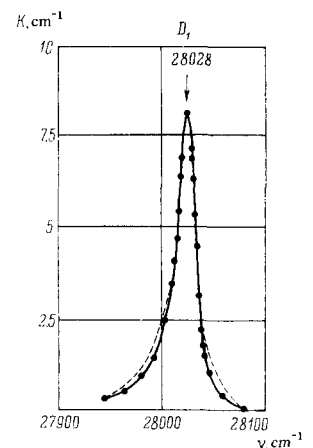


FIG. 13. Shape of asymmetrical D_1 band (${}^6A_{1g}({}^6S) \rightarrow {}^4T_{2g}({}^4D)$ transition) in the spectrum of MnF_2 ($T = 20.4^\circ \text{K}$) [24]. The dashed line shows a Lorentz curve with asymmetry $\alpha = -0.33$.

tron-magnon bands and comparison with data on neutron scattering make it possible even to estimate the width of the exciton band connected with the excitation of the 3d excitons.^[60,51] In the case of MnF_2 , the width of the exciton band $\Delta_{\text{exc}} \approx 2 \text{ cm}^{-1}$,^[50] which is comparable with the magnitude of the Davydov splitting in Cr_2O_3 .^[39]

The validity of the exciton model for the description of the exciton states of antiferromagnetic crystals with rutile structure (MnF_2 , FeF_2 , and CoF_2) was demonstrated in the reviews of Sell, Greene, and White^[51] and Loudon.^[52]

II. ABSORPTION OF LIGHT IN MAGNETICALLY ORDERED CRYSTALS

This chapter is devoted to an investigation of optical-spectrum singularities connected with antiferromagnetism of crystals. We shall discuss in succession the changes of the electron spectrum under the influence of exchange interaction, the change of the shape and width of the absorption bands due to electron-magnon interaction. The question of the participation of magnons in the absorption of light will be considered in detail.

6. Influence of Magnetic Ordering on the Structure of the Electronic Spectrum (Exchange Splitting of Energy Levels)

The influence of magnetic ordering on the structure of the spectrum becomes obvious from a group-theoretical analysis. Indeed, the symmetry of a magnetically-ordered crystal is defined as the intersection of the groups of the crystal and the magnetic moment. This, as a rule, leads to a lowering of the local symmetry for the absorbing ion and to a splitting of the absorption bands.

However, when the crystal goes over into the magnetically-ordered state, one should not expect considerable changes in the spectrum, since the exchange energy for the majority of antiferromagnetic compounds is of the order of 100 cm^{-1} , and the energy of the optical transition is 10^3 – 10^4 cm^{-1} (infrared region) or 10^4 – 10^5 cm^{-1} (visible and ultraviolet regions). Nonetheless, ordering may be accompanied by a noticeable change in the fine structure of the spectrum. Sugano and Tanabe^[53] proposed to explain the influence of the exchange interaction on the electronic spectrum of magnetically-ordered crystals from the point of view of the molecular-field theory; this is a rather crude approximation but explains many experimental results.

From the point of view of the molecular-field theory, the influence of the ordering on the spectral lines reduces to a consideration of the Zeeman effect in the effective exchange-interaction field

$$H_E = \frac{6kT_N}{Ng^2\mu_B} \frac{M_i}{S(S+1)}, \quad (6.1)$$

where T_N is the Neel temperature, N is Avogadro's number, g is the Lande factor, μ_B is the Bohr magneton, S is the spin of the magnetic ion, and M_i is the sublattice magnetization. At $T = 0^\circ\text{K}$, the maximum value is reached:

$$H_E = \frac{3kT_N}{g\mu_B(S+1)}. \quad (6.1')$$

It should be noted that H_E acts only on the spin of the

ion. If the ion has a total angular momentum J differing from the spin, then it is acted upon by a certain effective field H_{eff} , which is connected with the exchange field by the relation

$$H_{\text{eff}} = 2 \frac{g_J - 1}{g_J} H_E. \quad (6.2)$$

H_{eff} is in general anisotropic and depends on the orientation of the sublattice magnetizations relative to the crystallographic axes: $H_{\text{eff}} = \lambda M_i$. The latter circumstance can lead to anisotropy of the internal Zeeman effect upon reorientation of the sublattices by an external field. The splitting of the light absorption lines in a magnetically ordered crystal was observed in the case of europium iron garnet^[54,55] and the antiferromagnetic crystals Cr_2O_3 ^[39,56] and $\text{Dy}_3\text{Al}_5\text{O}_{12}$.^[57]

Most investigated antiferromagnets, however, are characterized not by splitting but by shifting of the absorption bands as a result of magnetic ordering (usually towards the short-wave side). This circumstance can be understood by taking into account the difference in the populations of the Zeeman components of the ground level of the ion, which is split in the field H_{eff} at low temperatures. The simplest case is when the Zeeman splitting of the excited-state level is very small compared with the splitting of the ground term. Since at low temperatures ($T \ll T_N$) only the lowest component of the ground level is populated, and the splitting of the excited state can be neglected, the shift of the absorption band by an amount determined by expression (6.1') becomes obvious. Such a simple case is realized in the antiferromagnetic compounds of nickel: NiF_2 ,^[21,59] KNiF_3 ,^[60] NaNiF_3 ,^[61,62] RbNiF_3 ,^[63] and also NiCl_2 .

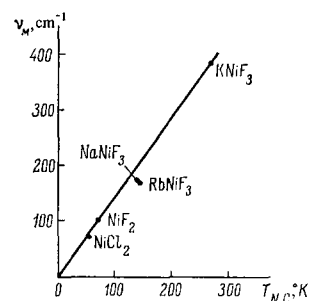


FIG. 14. Plot of the value $\nu_M = g\mu_B H_E$ of the exchange splitting of the Ni^{2+} ion vs. the magnetic-ordering temperature in the following crystals: KNiF_3 [60], RbNiF_3 and NaNiF_3 [64], NiF_2 [21], and NiCl_2 .

The effective exchange-interaction field splits the ground level of the Ni^{2+} ion, 3A_2 , into three components with $m_S = -1, 0$, and $+1$. When $T \ll T_N$, only the component with $m_S = -1$ is populated, and its energy is lower by an amount $g\mu_B H_E$ relative to the 3A_2 level in the paramagnetic phase ($T > T_N$). On the other hand, the splitting of an excited level, say 1E , vanishes in the first approximation. Consequently, the observed shift of the absorption band of Ni^{2+} is determined by the splitting of the 3A_2 level and is equal to $\nu_M = g\mu_B H_E$. In accordance with (6.1'), $\nu_M \sim T_N$, which is in good agreement with the experimental data shown in Fig. 14.

A sharp change of the absorption-band frequency following magnetic ordering was observed also for many antiferromagnetic compounds of manganese and cobalt: $\text{MnCl}_2 \cdot 4\text{H}_2\text{O}$,^[65] $\text{MnBr}_2 \cdot 4\text{H}_2\text{O}$,^[65] MnF_2 ,^[24, 66, 67] MnCO_3 ,^[48, 47] CoCO_3 ,^[46] CoF_2 ,^[14-16, 28, 46] and CoCl_2 .^[15, 29] This shift is illustrated in Fig. 15 with MnCO_3 as an example.

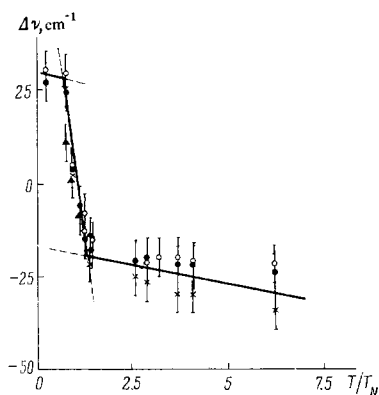


FIG. 15. Shift of light absorption frequencies in MnCO_3 following magnetic ordering [49]. X, ● — doublet ${}^6A_{1g}({}^6S) \rightarrow {}^4A_{1g}, {}^4E_g({}^4G)$; ▲, ○ doublet ${}^6A_{1g}({}^6S) \rightarrow {}^4T_{2g}({}^4D)$.

In the case of Mn^{2+} and Co^{2+} the situation is somewhat more complicated than in the case of Ni^{2+} . For these ions, the spin differs from zero also in the excited states, which are therefore split following the magnetic ordering and complicate the behavior of the absorption band frequencies near T_N . However, the shift of all the absorption bands in the spectrum of one and the same crystal is practically the same, in spite of the fact that the bands are due to transitions to different excited states (see Fig. 15). On the other hand, the magnitude of the shift is directly proportional to the Neel temperature of the crystal T_N .^[20] The observed connection between $\Delta\nu$ and kT_N is in good agreement with the conclusions of the theory of Tanabe and Sugano. The fact that the shift of all the absorption bands in the spectrum of one and the same crystal is practically the same offers evidence that the splitting of the excited-state levels in the field H_{eff} is much smaller than the splitting of the ground state. This question was discussed by Stout^[66] with MnF_2 as an example. In the case of total magnetic ordering ($T = 0$), both the ground and the excited states of Mn^{2+} are split in the effective field H_{eff} . The interval between two neighboring Zeeman components with m_S and $m_S + 1$ is equal to $g\mu_B H_{\text{eff}}$ (6.1'). One must, however, take into account the fact that the exchange interaction in the compounds under consideration has an indirect superexchange character, in which the nonmagnetic ions F^- , Cl^- , and Co_3^{2-} take part. For MnF_2 , the separation of each mechanism is realized as a result of the overlap of the d orbitals of Mn^{2+} with the neighboring F^- ions. Since the Mn^{2+} ion in the MnF_2 is in the center of an octahedron made up of chlorine ions, the overlap is the largest for the $d\gamma$ orbitals. The exchange integral is therefore proportional to the population of the $d\gamma$ orbitals by electrons with a spin oriented along the C_4 axis of the crystal. According to Stout,^[66] this population is not the same for different states of Mn^{2+} , and amounts to $1/5$ for the ground ${}^6A_{1g}$ state, $2/15$ for ${}^4A_{1g}({}^4G)$, $4/21$ for ${}^4E_g({}^4G)$, and $1/7$ for ${}^4E_g({}^4D)$. Thus, the exchange integral, and consequently also H_{eff} , should not greatly change on going over from the ground state to the excited state (this change amounts to 20–30% for different excited states), and the differences between the exchange energies and the states under consideration

are determined mainly by the value of the spin. When account is taken of the figures given above for the $d\gamma$ -orbit populations, the energies of the exchange interaction in different states with a surrounding of unexcited ions should be in the ratio $5/2 \times 1/5) : (3/2 \times 2/15) : (3 \times 2 \times 4/21) : (3/2 \times 1/7)$. Thus, the levels of all the excited states of the Mn^{2+} ions, whose spins ($3/2$) are smaller than the spin of the ground state ($5/2$), are shifted much less by the magnetic ordering than the ground levels, and the shifts of the levels of all the excited states can be assumed the same within 20% accuracy. Consequently, in the first approximation it can be assumed that the shifts of all the Mn^{2+} bands in the case of antiferromagnetic ordering are due to different changes of the energy of the ground and excited states, in view of the fact that their spins are different, while the effective field H_{eff} can be regarded as being the same for all the states.

A similar conclusion was reached by Tsujikawa and Kanda,^[65] who investigated manganese bromide and chloride. In the interpretation of their results they have also assumed that H_{eff} is the same in the ground and in the excited states of the manganese. In this case, the shift of the ground-state level of Mn^{2+} following magnetic ordering is $(5/2)g\mu_B H_{\text{eff}}$, and that of the excited level is $(3/2)g\mu_B H_{\text{eff}}$, and consequently the shift of the absorption bands should be $g\mu_B H_{\text{eff}}$. Using the experimentally observed quantities (0.9 cm^{-1} for the chloride and 1.5 cm^{-1} for the bromide), it is possible to estimate H_{eff} . The values of H_{eff} obtained by such an estimate (9,000 Oe for the chloride and 16,500 Oe for the bromide) are in good agreement with the results of investigations of the magnetization. Within the framework of such an approximation, it is also easy to understand why the absorption bands due to transitions between states with identical spins do not experience an anomalous shift in the case of magnetic ordering (the B band and CoCO_3 ,^[48] the infrared band $\nu \approx 7,000 \text{ cm}^{-1}$ in CoF_2 and CoCl_2 ^[14,28]).

However, such a simplified approach turns out to be highly inadequate for the explanation of the anomalous behavior of the absorption bands of the antiferromagnetic crystals CoF_2 and CoCl_2 in the infrared region ($800\text{--}2,000 \text{ cm}^{-1}$). Figure 16a shows the temperature dependence of the frequency shift of two infrared absorption bands in the CoF_2 spectrum. It is important that both bands experience an anomalous frequency shift towards the long-wave side when the crystal is cooled below T_N , and the magnitude of the shift is different in the two bands investigated in detail (1345 and 1295 cm^{-1} —their frequencies at 15°K). On the other hand, the band $\nu = 1006 \text{ cm}^{-1}$ ($T = 15^\circ\text{K}$) in CoCl_2 (Fig. 16b) shifts in the T_N region to the short-wave side when the temperature is decreased. These facts can be explained when account is taken of the detailed identification of the infrared-absorption bands of CoCl_2 and CoF_2 , which was mentioned earlier (Sec. 3). We shall regard the exchange splitting as the result of the Zeeman effect in an effective field H_{eff} . However, in the case of Co^{2+} it is necessary to take into account the fact^[14] that the low-symmetry crystal field and the spin-orbit interaction cause the wave function to be superpositions of states with different orbital m_l and spin m_s quantum numbers. In

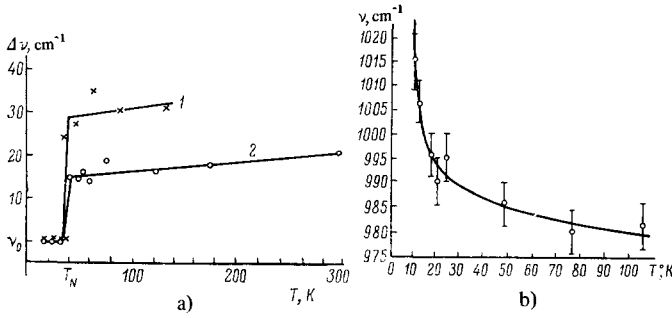


FIG. 16. Temperature dependence of the frequency shift of the infrared absorption bands in: 1) CoF_2 (1 - 1345 cm^{-1} band, 2 - 1285 cm^{-1} band [16]), b) CoCl_2 (1006 cm^{-1} band) ($T = 15^\circ\text{K}$) [20].

this case H_{eff} acts on the total angular momentum. It is assumed that the field H_{eff} is the same for all the states, and the operator of interaction with it has the same form as for the external field:^[12]

$$\hat{\mathcal{H}} = \mu_B H_{\text{eff}} \left(-\frac{3}{2} \hat{L}_z + 2\hat{S}_z \right). \quad (6.3)$$

Then the Zeeman splitting of the Kramers doublet Ψ_i^\pm is determined by the expression

$$\Delta E = \langle \Psi_i^\pm | \left(-\frac{3}{2} \hat{L}_z + 2\hat{S}_z \right) | \Psi_i^\pm \rangle \mu_B H_{\text{eff}}. \quad (6.4)$$

On the other hand, we can write

$$\Delta E = 2g_{\text{eff}} \mu_B H_{\text{eff}} S. \quad (6.5)$$

The anisotropy of the Zeeman effect can be taken into account by introducing the anisotropic g_{eff} factor, which can be determined by equating (6.4) with (6.5) for an effective spin $S = 1/2$.

If the z direction coincides with the C_3 axis of the CoCl_2 crystal, then the magnetic-field operator takes the form

$$\hat{\mathcal{H}}_{11} = \mu_B H_{\text{eff}} \left(-\frac{3}{2} \hat{L}_z + 2\hat{S}_z \right). \quad (6.6)$$

Assuming that the anisotropy of H_{eff} in the basal plane of CoCl_2 is very small (as is confirmed by measurements of the magnetic susceptibility), we write down the magnetic-field operator for this direction

$$\hat{H}_\perp = \mu_B H_{\text{eff}} \left[\frac{3}{2} (\hat{L}^+ - \hat{L}^-) + 2(\hat{S}^+ - \hat{S}^-) \right], \quad (6.7)$$

where

$$\hat{L}^+ = \hat{L}_x + i\hat{L}_y, \quad \hat{L}^- = \hat{L}_x - i\hat{L}_y.$$

The values of g_{eff} calculated on the basis of the foregoing expressions for the levels ($E_1 - E_6$) of the lowest triplet ${}^4T_{1g}({}^4F_{g/2})$ of the Co^{2+} ion, which determine the infrared absorption spectrum of CoCl_2 in the $600-2,000 \text{ cm}^{-1}$ region, are given in [14]. Since the magnetic moments in CoCl_2 lie in the basal plane of the crystal, we confine ourselves to the case $H_{\text{eff}} \perp C_3$ and assume that H_{eff} is the same for all the levels E_i ($i = 1-6$). Judging from the values of the g factors, the greatest splitting after magnetic ordering should be experienced by the ground level E_1 . The levels E_2 , E_5 , and E_6 are not split at all in the linear approximation. Thus, we can expect CoCl_2 infrared bands connected with the transitions in question to experience a short-wave shift following

magnetic ordering. Such a picture agrees qualitatively with the results of the experiments (see Fig. 16b).

In the case of CoF_2 , Lines^[68] calculated the splitting of the two lowest levels of Co^{2+} under magnetic ordering of the crystal. Even in this simple case, it was necessary to introduce a number of anisotropic parameters, the values of which were chosen such as to obtain the best agreement between calculation and experiment. The extension of such a calculation to the case of a large number of levels involves an increase in the number of the adjustment parameters and affects the uniqueness of the results. It is possible to employ the procedure described above. To explain the long-wave shift of the infrared bands of CoF_2 in this case, however, it was necessary to make the additional assumption that H_{eff} is different in the ground and excited states of Co^{2+} .^[14] Attention is called to the fact that the absorption-band shift due to the exchange interaction is observed not only near the magnetic ordering temperature, but also considerably above it. This gives grounds for assuming that the change in the electronic spectrum is due to the appearance of a short-range magnetic order. A similar conclusion that the singularities of the optical-spectrum structure of antiferromagnets is connected with short-range magnetic order was arrived at by Cooke et al.,^[69] who investigated the absorption spectrum of the antiferromagnetic garnet $\text{Dy}_3\text{Al}_5\text{O}_{12}$ ($T = 2.49^\circ\text{K}$). Using the band $\lambda = 3649 \text{ \AA}$ as an example, they succeeded in demonstrating that the temperature dependence of the frequency shift of this band is similar to a temperature dependence of the magnetic energy, obtained by integrating the magnetic part of the specific heat of $\text{Dy}_3\text{Al}_5\text{O}_{12}$, and does not coincide with the temperature dependence of the sublattice magnetization.

The conclusion that a major role is played in the formation of the optical and infrared spectrum singularities is played by the short-range magnetic order is confirmed by the results of an investigation of the light absorption spectra in antiferromagnetic crystals containing transition-group impurity ions in addition to the main ions. In spite of the fact that this changes greatly the structure of the crystal spectrum, it is possible to identify the absorption band with optical transitions of the magnetic ions contained in both the matrix crystal and in the impurity ions—for the system $x\text{MnF}_2 - (1-x)\text{CoF}_2$. The temperature dependence of the absorption-band frequencies of the antiferromagnetic-crystal impurity ions, as shown by experiment, is determined by the magnitude of the exchange interaction between them and the magnetic ions of the matrix.^[70-72]

7. Anisotropy of Exchange Splitting of the Energy Levels

As noted above (Sec. 6), the exchange splitting of the energy levels can be anisotropic for states with appreciable spin-orbit interaction. The first to observe the anisotropy of exchange splitting of the energy levels of Yb^{3+} in the exchange field of iron ions in ytterbium iron garnet was Wickersheim,^[78] with the $E_{5/2}({}^2F_{7/2}) \rightarrow E_{5/2}({}^2F_{5/2})$ transition as an example. In this case the structure of the exchange splitting could be easily changed by rotating the spontaneous magnetic moment of the crystal relative to the crystallographic axes with the aid of relatively weak external magnetic fields. The

experimental results have made it possible to determine the exchange splittings of the doublets of the ground and excited states as functions of the orientation of the effective exchange-interaction field. On the basis of the similarity between the exchange splitting of the ground state and the splitting and the external field, observed with the aid of paramagnetic resonance of ytterbium in gallium and aluminum garnets, Wickersheim proposed that the exchange splittings of this doublet can behave in exactly the same manner as the g-tensor of a two-level system, i.e., the splitting has the following form:

$$\Delta E = [(\Delta E_x)^2 l^2 + (\Delta E_y)^2 m^2 + (\Delta E_z)^2 n^2]^{1/2} \quad (7.1)$$

where ΔE_x , ΔE_y , and ΔE_z are the principal values and l , m , and n are the direction cosines of the exchange field relative to the principal axes of the system ($\Delta E_i = g\mu_B H_{\text{eff}, i}$, $i = x, y, z$). For the ytterbium iron garnet ion with an exchange field bounded by the plane (110), for example, there are four nonequivalent sites, and the exchange splittings of the doublets are given by the relations

$$\begin{aligned} \Delta E_1 &= [\Delta E_x^2 \cdot \cos^2 \theta + \Delta E_y^2 \cdot \sin^2 \theta]^{1/2}, \\ \Delta E_2 &= [\Delta E_x^2 \cdot \cos^2 \theta + \Delta E_z^2 \cdot \sin^2 \theta]^{1/2}, \\ \Delta E_3 &= \left[\Delta E_x^2 \cdot \frac{\sin^2 \theta}{2} + \Delta E_y^2 \left(\frac{\cos^2 \theta}{2} + \frac{\sin^2 \theta}{4} + \frac{\sin \theta \cdot \cos \theta}{\sqrt{2}} \right) + \right. \\ &\quad \left. + \Delta E_z^2 \left(\frac{\cos^2 \theta}{2} + \frac{\sin^2 \theta}{4} - \frac{\sin \theta \cdot \cos \theta}{\sqrt{2}} \right) \right]^{1/2}, \\ \Delta E_4 &= \left[\Delta E_x^2 \cdot \frac{\sin^2 \theta}{2} + \Delta E_y^2 \left(\frac{\cos^2 \theta}{2} + \frac{\sin^2 \theta}{4} - \frac{\sin \theta \cdot \cos \theta}{\sqrt{2}} \right) + \right. \\ &\quad \left. + \Delta E_z^2 \left(\frac{\cos^2 \theta}{2} + \frac{\sin^2 \theta}{4} + \frac{\sin \theta \cdot \cos \theta}{\sqrt{2}} \right) \right]^{1/2}, \end{aligned} \quad (7.2)$$

where θ is measured relative to the [100] direction in the (110) plane. Using the known values of the g-tensor for ytterbium in ytterbium-gallium garnet and the experimentally obtained exchange splittings, Wickersheim succeeded in determining the principal values of the effective magnetic fields H_{eff} , and consequently, in accordance with formula (6.2), also the exchange fields for the ground state of the ytterbium ion, which are equal to 349, 611, and 678 kOe along the x, y, and z axes, respectively. If the g-tensor for the excited state is known, say from the optical Zeeman effect, then it is possible to determine the effective magnetic field for the excited state of the rare-earth ion. On the basis of the experimental data,^[73] Levy^[74] and Koster (see^[75]) advanced the hypothesis that the exchange interaction between the rare-earth ions and iron cannot be described by an isotropic interaction of the Heisenberg type.

G. S. Krinchik and M. V. Chetkin^[76] were the first to notice the connection between the polarization of the absorption bands in the orientation of the magnetization vector of iron garnet. Inasmuch as the splitting of the lines is determined by the orientation of the magnetic sublattices relative to the crystallographic axes,^[73] it is natural that the mutual orientation of H_ω and M_i in the case of magnetic dipole transitions, and of E_ω and M_i in the case of electric dipole transitions, determines the relative intensity of the Zeeman components. This has been confirmed experimentally and has made it possible to justify the optical method of investigating magnetic anisotropy, which we shall illustrate with erbium iron garnets $\text{Er}_3\text{Fe}_5\text{O}_{12}$ as an example.

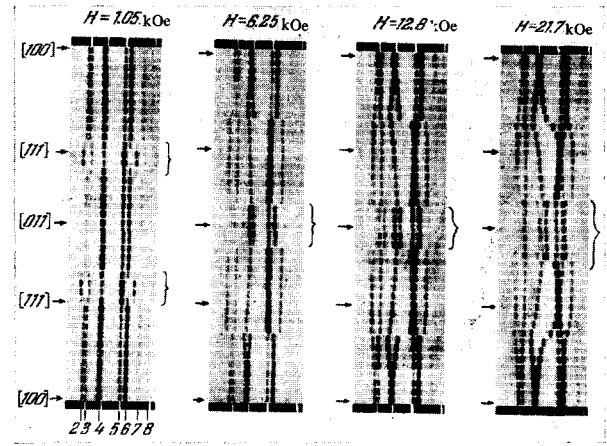


FIG. 17. Anisotropy of exchange splitting in the region of the ${}^4I_{15/2} \rightarrow {}^4S_{3/2}$ transition of the Er^{3+} ion in erbium iron garnet ($T = 4.2^\circ\text{K}$)^[77].

In one of our investigations we study in detail in the anisotropy of the exchange splitting in the region of the ${}^4I_{15/2} \rightarrow {}^4S_{3/2}$ transition of the absorption spectrum of Er^{3+} in erbium iron garnet.^[77,78] In Fig. 17 we can see, even in a weak magnetic field, a jumplike change of the spectrum at definite values of the angle φ between the easy-magnetization axis [100] and the external field H . A detailed investigation of the dependence of the structure of the exchange splitting on the intensity of the external magnetic field has shown that appreciable magnetic fields are necessary to saturate the magnetic moment M_S along an arbitrary direction in the plane of the sample. An external magnetic field H sufficient to overcome the anisotropy energy of the iron garnet, when deflected from the [100] axis, drags with it the moment M_S , but the latter does not become parallel to the field and makes an angle θ with the [100] direction. Investigations in polarized light have shown that to each direction of the external magnetic field in the plane of an erbium iron garnet plate there correspond two mutually perpendicular directions of the electric vector E_ω of the linearly polarized light, at which the polarized bands of the ${}^4I_{15/2} \rightarrow {}^4S_{3/2}$ transition have an extremal intensity. Figure 18 shows the spectra corresponding to the best

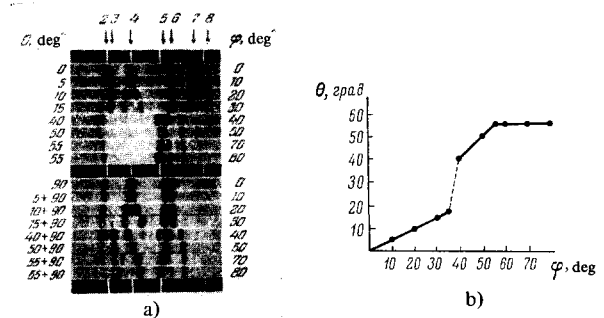


FIG. 18. a) Absorption spectrum of Er^{3+} in polarized light. The angle between the vector E of linearly polarized light and the [100] axis corresponds to the extremal intensity of the polarized absorption bands. $0 \ll \varphi \ll 80^\circ$ ($H = 21.7 \text{ kOe}$, $T = 4.2^\circ\text{K}$). b) Dependence of the angle θ between the magnetization vector M_S and the [100] axis on the angle φ between the external magnetic field H and the [100] axis ($H = 21.7 \text{ kOe}$, $T = 4.2^\circ\text{K}$)^[77]

polarization of the lines at different orientations of the external field (a), and also the connection between the angles θ and φ (b). Knowing the angles θ and φ it is easy to determine the first and second constants of the magnetic crystallographic anisotropy of erbium iron garnet. To this end, we write down the free energy of the ferromagnetic crystal as the sum of the anisotropy energy and the energy in the external field, confining ourselves to the constants K_1 and K_2 :

$$W = W_a + W_H = K_1(\alpha_1^2\alpha_2^2 + \alpha_2^2\alpha_3^2 + \alpha_3^2\alpha_1^2) + K_2\alpha_1^2\alpha_2^2\alpha_3^2 - H I_S. \quad (7.3)$$

If \mathbf{H} lies in the (110) plane we have $\alpha_1 = \cos \theta$ and $\alpha_2 = \alpha_3 = (\sqrt{2}/2) \sin \theta$, and Eq. (7.3) takes the simpler form

$$W = \frac{1}{4} K_1 (\sin^4 \theta + \sin^2 2\theta) + \frac{1}{16} K_2 \sin^2 2\theta - I_S H \cos(\varphi - 0). \quad (7.4)$$

The experimentally measured equilibrium angle θ is given by the equation

$$\frac{\partial W}{\partial \theta} = 0. \quad (7.5)$$

Using the values of θ obtained with the aid of the proposed optical method, the known value of the saturation magnetization $I_S = 20 \mu_B/\text{mole}$, and the unit-cell parameter $a = 12 \text{ \AA}$, we obtain $K_1 = 9 \times 10^6 \text{ erg/cm}^3$ and $K_2 = 5 \times 10^7 \text{ erg/cm}^3$. These agree with the data obtained by the traditional magnetic methods.

Since anisotropy of the exchange splitting is to be expected only for states with appreciable spin-orbit interaction,^[74] in the case of manganese compounds this anisotropy is connected with the splitting of the excited states, since the ground state is ${}^6S_{5/2}$ ($L = 0$). The simplest example to understand is that of a uniaxial collinear antiferromagnet. In this case, an external magnetic field oriented along the principal crystallographic axis C_n turns over the magnetic moments of the sublattices when a critical intensity $H_C = \sqrt{2H_E H_A}$ is reached (H_A —magnetic anisotropy field, H_E —exchange field), so that the magnetic moments change their orientation jumpwise from $\mathbf{M}_i \parallel C_n$ to $\mathbf{M}_i \perp C_n$. The turning of the magnetic sublattices is accompanied by an abrupt change in the structure of certain optical transitions (the "threshold" Zeeman effect). Such an effect was observed by Stager^[79] in the spectrum of Cr_2O_3 ($H_C = 60 \text{ kOe}$) and by one of authors^[80,81] in the spectrum of MnF_2 ($H_C = 95 \text{ kOe}$). In the case of MnF_2 , the "threshold" Zeeman effect is observed only in the region of the ${}^6A_{1g}({}^6S) \rightarrow {}^4T_{1g}({}^4D)$ transition (Fig. 19) and has a sharply pronounced anisotropy (Fig. 20). The "threshold" Zeeman effect is interpreted on the basis of a calculation of the exchange splitting of the energy levels with allowance for the spin-orbit interaction. It turns out that the g factor is anisotropic in a rhombic crystal field (the case of MnF_2) only for states that are characterized by the 4T_g representation in the O_n group. Therefore changes in the spectrum structure following rotation of the magnetic sublattices are observed only for the D group of the MnF_2 bands connected with the transition to the excited state ${}^4T_{1g}({}^4D)$, and the structure of the remaining groups is not changed, since their g -factor is isotropic.

The behavior of the electric dipole absorption bands of MnF_2 in an external magnetic field can be regarded as unique proof of the exciton mechanism of light absorption in magnetically-concentrated crystals, or at

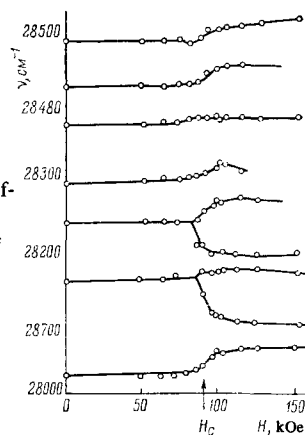


FIG. 19. "Threshold" Zeeman effect in MnF_2 for bands in the region ${}^6A_{1g}({}^6S) \rightarrow {}^4T_{1g}({}^4D)$ transitions ($T = 20^\circ\text{K}$) [81]. \mathbf{H} is parallel to the tetragonal axis.

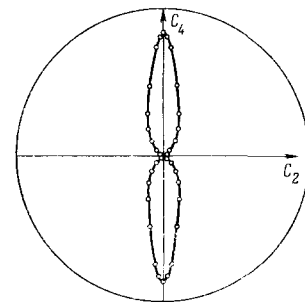


FIG. 20. Anisotropy of the "threshold" Zeeman effect for the MnF_2 band $\nu = 28238 \text{ cm}^{-1}$ ($T = 20^\circ\text{K}$) [20].

least in MnF_2 . Indeed, while an external magnetic field \mathbf{H} oriented along the C_4 axis and smaller in intensity than the critical field $H_C = 95 \text{ kOe}$, does not split the levels of the individual ions (the local symmetry is D_{2h} , and the Kramers degeneracy is lifted by the exchange field H_E), it does increase the energy of the ions in one sublattice ($+g\mu_{\text{eff}}SH$) and decreases that of the other ($-g\mu_{\text{eff}}SH$). For the manganese ion, for example, the spin of the ground state $S = 5/2$ ($-5/2$) differs from the spin of the excited state $S^1 = S - 1 = 3/2$ ($-3/2$). In an external magnetic field, the band corresponding to excitation of the ion of one sublattice shifts by an amount $[g\mu_{\text{eff}}HS - g'\mu_{\text{eff}}H(S-1)]$, while for the ion of the second sublattice it shifts by $[-g\mu_{\text{eff}}HS + g'\mu_{\text{eff}}H(S-1)]$, i.e., the line corresponding to the transition between the considered states is split in an external magnetic field H symmetrically by an amount

$$\Delta = 2\mu_{\text{eff}}H [gS - g'(S-1)]. \quad (7.6)$$

Consequently, if the transitions were localized, then a Zeeman splitting of the bands would be observed in a field $H < H_C$, owing to the lifting of the sublattice degeneracy. On the other hand, the exciton absorption bands connected with the collective excitations cannot split if $\mathbf{H} \parallel C_4$ and is lower in intensity than H_C , for in this case the symmetry of the crystal does not change. The splitting of the exciton bands is possible when H_C is reached, since the magnetic symmetry of the crystal, defined as the intersection of the factor group D_{2h} and the magnetic-moment group $C_{\infty h}$ changes strongly when the sublattices are turned. It is precisely under these conditions that the "threshold" Zeeman effect of the electric dipole bands of MnF_2 is observed, thus demonstrating their exciton nature. The absence of an influence of the external magnetic field up to 190 kOe on

other electric dipole transitions in MnF_2 (${}^6\text{A}_{1g}({}^6\text{S}) \rightarrow {}^4\text{A}_{1g}({}^4\text{G})$ and ${}^6\text{A}_1({}^6\text{S}) \rightarrow {}^4\text{E}({}^4\text{D})$)^[81] likewise does not contradict the assumption that they have an exciton nature. As to the weak magnetic dipole absorption bands, their behavior in an external field can be correctly interpreted by means of the single-ion model. In^[82] they observed a Zeeman splitting of weak magnetic dipole absorption lines E1 (18419.6 cm^{-1}) and E2 (18436.6 cm^{-1}) for the transition ${}^6\text{A}_{1g}({}^6\text{S}) \rightarrow {}^4\text{T}_{1g}({}^4\text{G})$ of MnF_2 in a field $H < H_c$, oriented along the tetragonal C_4 axis, which was interpreted as a result of lifting of the sublattice degeneracy in the external magnetic field H . The validity of such an analysis was subsequently corroborated by Sell et al.^[51] According to their analysis, the result does not mean that the E1 and E2 bands are not due to exciton effects, since splitting due to the lifting of the sublattice degeneracy is possible within the framework of the collective (exciton) model if the excitation migrates only over ions situated in one of the sublattices. Sell et al.^[51] have shown theoretically that such a situation can be realized in the case of MnF_2 for purely electronic excitations. They considered a rather simplified model consisting of N unit cells, each of which contains two non-equivalent magnetic ions, and each ion has h optically active electrons. The influence of the phonons is neglected. The system has only two energy levels: the ground level $g_{n\mu}$ and the excited one $e_{n\mu}$. In the zeroth approximation, the ions do not interact, and each ion is described by a Hamiltonian $\mathcal{H}_{n\mu}$, where $n\mu$ pertains to the μ -th position of the ion in the n -th unit cell. Then the wave function of the ground state of the entire crystal is given by

$$|G\rangle = |A \prod_n \prod_{\mu=1}^2 g_{n\mu}\rangle, \quad (7.7)$$

and for a state in which the n -th ion is excited

$$|E_{n\mu}\rangle = |A e_{n\mu} \prod_{j \neq n\mu} g_{j\nu}\rangle, \quad (7.8)$$

where A is the operator that antisymmetrizes the wave functions of the crystal. If we now turn on the energy $V_{n\mu, j\nu}$ of the interaction between the $n\mu$ -th and $j\nu$ -th ions, then the Hamiltonian of the entire crystal is

$$\mathcal{H} = \sum_{n=1}^N \sum_{\mu=1}^2 \mathcal{H}_{n\mu} + \frac{1}{2} \sum_{n, j=1}^N \sum_{\mu, \nu=1}^2 V_{n\mu, j\nu}. \quad (7.9)$$

The matrix elements of the Hamiltonian

$$\langle E^{\mu\mathbf{k}} | \mathcal{H} | E^{\nu\mathbf{k}} \rangle = \delta_{\mu\nu} W(E) + V_{\mu\nu}(\mathbf{k}) \quad (7.10)$$

are the energies of the crystal with one excited ion. Then

$$W(E) = \langle E_{01} | \mathcal{H} | E_{01} \rangle \quad (7.11)$$

characterizes the so-called energy shift of the band. The diagonal term

$$V_{11}(\mathbf{k}) = \sum_{n=1}^N \langle e_{n1} g_{01} | V_{n1, 01} | P g_{n1} e_{01} \rangle \cos(\mathbf{k}\mathbf{r}_{n1}) \quad (7.12)$$

and the non-diagonal term

$$V_{12}(\mathbf{k}) = \sum_{n=1}^N \langle e_{n2} g_{01} | V_{n2, 01} | P g_{n2} e_{01} \rangle \cos(\mathbf{k}\mathbf{r}_{n2}) \quad (7.13)$$

determine the excitation transfer between ions of one sublattice and ions of opposite sublattices respectively; P is the perturbation operator.

In MnF_2 , all the narrow-band optical transitions are spin-forbidden. For such transitions, the inter-sublattice coupling $V_{12}(\mathbf{k})$ is negligibly small, as follows intuitively from the results of Moriya,^[83] namely, for spin-forbidden transitions, the z -component of the total spin momentum changes by 2 whenever the excitation goes over from one sublattice to another, a fact forbidden by the momentum conservation requirement. Such a process calls for a ground-state spin-orbit coupling that is weak compared with the intrasublattice interaction in the case of Mn^{2+} ions. The same conclusion is obtained when the values of $V_{11}(\mathbf{k})$ and $V_{12}(\mathbf{k})$ are estimated.^[51]

In the case when $V_{12} = 0$, the properties of the excitons simplify greatly. This leads to the consequence that the sublattice states become eigenstates of the system. The excitation thus belongs to equivalent states, whereas the general case is equally distributed among two non-equivalent sublattices. It is easy to see that no exciton effects will be observed for purely electronic absorption, such as the E1 and E2 ions. Since the light has a large wavelength, the momentum conservation law calls for the momentum of the produced exciton be equal to zero. There can be no Davydov splitting, since $V_{12}(0) \sim 0$. Thus, the main basis for describing purely electronic absorption by the single-ion model is the fact that the excitation belongs to one sublattice.

The considered two-level model obviously holds for Mn^{2+} ions, which have many excited states in the $3d^5$ configuration, only in the first-order approximation (but a higher-order approximation leads to great complications). This approximation is not fully applicable even to the exciton bands connected with the E1 and E2 lines, since these bands have practically the same energy, although in this case this approximation apparently holds true. To obtain satisfactory agreement with experiment for all the transitions in MnF_2 , one apparently cannot consider the collective model independently for each excited state of Mn^{2+} while neglecting the coupling between the nondegenerate ion states, since the mixing between these states can obviously be appreciable.

However, the foregoing analysis of the Zeeman effect for bands of different nature in MnF_2 leads to the following conclusion: Weak magnetic dipole transitions, which are allowed in the crystal as a result of the spin-orbit interaction, can be described by the single-ion model. Conversely, strong electron dipole transitions, which become allowed in the crystal by a much more complicated mechanism (Secs. 3 and 8) are described by the collective (exciton) model.

8. Magnon Participation in Light Absorption

Magnetic ordering of crystals produces, besides the already considered change in the electron spectrum as a result of exchange splitting of the levels of the unfilled ion shells, also a new energy branch connected with excitation of oscillations of the magnetic moments. If we confine ourselves to the region of low temperatures $T < 0.3T_N$, then we are dealing with the magnon or spin-wave branch of the spectrum. For nonmagnetic crystals, the interaction of the electronic excitations with the crystal-lattice vibrations (electron-phonon

interaction) causes singularities in the form of the absorption bands and in the structure of the spectrum. In magnetically-ordered crystals, owing to the exciton-magnon and phonon-magnon interaction, new details of the structure and form of the absorption bands are also possible.

In this section we discuss the antiferromagnetic crystal spectrum-structure features connected with excitation of spin waves when light is absorbed. We shall consider in succession the possible mechanisms of light interaction with a spin system of a crystal in concrete regions of the spectrum: a) the far infrared region (two-magnon absorption), b) the infrared region (phonon-magnon absorption), and c) the visible and ultraviolet region (electron-magnon satellite bands).

a) Two-magnon absorption. In the investigation of the absorption spectrum of antiferromagnetic fluorides of the iron group, FeF_2 , MnF_2 , and CoF_2 , in the far infrared region of the spectrum, electric dipole absorption bands were observed at the frequencies 154.4, 110, and 120 cm^{-1} .^[84-88] The singular features of these bands made it possible to propose that they are connected with magnetic ordering of the crystal. Notice should be taken of the most characteristic features of this absorption, which were investigated in detail for the antiferromagnetic FeF_2 and MnF_2 : 1) the absorption band is sharply polarized, and the absorption is strongest when the electric vector is polarized along the tetragonal axis of the crystal. 2) The intensity of the band is maximal at $T \rightarrow 0$ and is comparable with the intensity of the antiferromagnetic resonance line. 3) When the temperature is increased, the band broadens and vanishes near the Neel temperature of the crystal. 4) The frequency of the band decreases less sharply than the frequency of the antiferromagnetic resonance line when $T \rightarrow T_N$. 5) The band is insensitive to an external magnetic field of intensity up to 50 kOe.

A similar absorption was recently observed by Richards^[89] for at the weak-ferromagnetism antiferromagnets NiF_2 and MnCO_3 . Unlike the previously considered easy-axis antiferromagnets, the two-magnon absorption is not observed in NiF_2 and MnCO_3 in a zero external field, and has a number of singularities that have not been investigated in detail either theoretically or experimentally. A comparison of the frequencies of the observed absorption bands for the case of FeF_2 and MnF_2 with the known neutron-diffraction investigations of the spin-wave dispersion in these crystals has made it possible to propose that they are connected with the absorption of light, wherein two short-wave spin waves are simultaneously created, with frequencies and wave vectors near the boundary of the Brillouin zone.

To explain the possibility of two-magnon absorption, is necessary to understand first how the electric field of the light wave interacts with spin waves in a magnetically-ordered crystal. As mentioned in Sec. 3, transitions within the limits of the $3d^n$ configuration are parity-forbidden in the electric-dipole approximation; the observed strong electric dipole absorption cannot be explained within the framework of the single-ion model. Electric dipole transitions become possible if two interacting ions take part simultaneously in the absorption. The theory of such a process with a case of solid was developed by Dexter.^[89] The two-magnon ab-

sorption mechanism described below can be regarded as a particular case of this theory. Independently of its concrete nature, the interaction between the pair of ions i and j should lead to allowance of such a transition, wherein the ion i changes its spin component by $\Delta S_i^z = -1$ and goes over into any odd (even) state of the free ion $|e\rangle$, whereas the neighboring ion j changes the spin component by $\Delta S_j^z = +1$, and remains in the ground orbital state $|g\rangle$. This leads to the appearance of an electric dipole moment, the interaction of which with the \mathbf{E}_ω vector of the light wave can be written in the form

$$\mathbf{E}_\omega \cdot \pi_{ij}^{eg} a_i^+ S_j^+ \quad (8.1)$$

where $a_i^+ = |e\rangle \langle g|$ is the transition operator between the states $|e\rangle$ and $|g\rangle$, and π_{ij}^{eg} is the dipole moment of the transition. Since the process in which the ion j goes over into the state $|e\rangle$ and the ion i remains in the ground state $|g\rangle$, is equally probable the Hamiltonian of the exciton-magnon electric dipole transition in the pair of ions i and j can be written in the form

$$\mathcal{H}_{ij}^{eg} = E_\omega \pi_{ij}^{eg} a_i^+ S_j^+ + E_\omega \pi_{ji}^{eg} a_j^+ S_i^+ \quad (8.2)$$

For the particular case when the final orbital state of the two ions is the ground state, and the only spin components change, the Hamiltonian is transformed into

$$\mathcal{H}_{ij}^{2\text{mag}} = E_\omega (\pi_{ij} + \pi_{ji}) S_i^- S_j^+ \quad (8.3)$$

since the exciton operators are in this case connected with the spin operators by the relations^[52]

$$a_i^- = \frac{S_i^-}{\sqrt{2S}}, \quad a_j^+ = \frac{S_j^+}{\sqrt{2S}} \quad (8.4)$$

and the denominator $(2S)^{1/2}$ is taken into account in the moment π . If we sum in the Hamiltonian (8.3) over all the ion pairs in the lattice and take into account only the interaction between the nearest neighbors in the opposite sublattices, a group-theoretical analysis with allowance for symmetry makes it possible to write in each concrete case the Hamiltonian of the two-magnon interaction; for example, for MnF_2 (FeF_2) it takes the form

$$\mathcal{H}^{2\text{mag}} = \sum_{\langle i,j \rangle} \{A E_x \sigma_{ij}^x + A^* E_y \sigma_{ij}^y + B E_z \sigma_{ij}^z \sigma_{ij}^z\} S_i^- S_j^+ \quad (8.5)$$

where A and B are simple combinations of the components π_{ij} and π_{ji} , and σ_{ij}^α ($\alpha = x, y, z$) takes on the values ± 1 , depending on the sign of the α component of the vector joining the ions i and j .

The spin Hamiltonian (8.5) is invariant against all operations of the magnetic-symmetry group of MnF_2 (FeF_2), including the time-reversal operation. Other symmetry-allowed terms of the Hamiltonian (8.5) do not lead to two-magnon absorption.

The absorption coefficient can be written in the form

$$\alpha_i(\nu) \sim \frac{\nu}{n} \int d^3k |M_i(\mathbf{k})|^2 \delta[\hbar\nu - 2E(\mathbf{k})] \quad (8.6)$$

where $M_i(\mathbf{k})$ is the matrix element of the electric dipole transition in which two magnons with opposite momenta are produced ($i = 1, 2$ corresponds to $\mathbf{E}_\omega \parallel \mathbf{C}$ and $\mathbf{E}_\omega \perp \mathbf{C}$), n is the refractive index, ν is the frequency of the absorbed photon, and $E(\mathbf{k})$ is the energy of the magnon with wave vector \mathbf{k} . In two-magnon absorption it is necessary to take into account the energy and momentum

conservation laws:

$$E_1(\mathbf{k}_1) + E_2(\mathbf{k}_2) = \hbar\nu, \quad \mathbf{k}_1 + \mathbf{k}_2 = \mathbf{Q} \approx 0; \quad (8.7)$$

here $\hbar\nu$ is the energy of the absorbed photon, $E_1(\mathbf{k}_1)$ and $E_2(\mathbf{k}_2)$ are the energies of the two magnons produced upon absorption of light, respectively, \mathbf{k}_1 and \mathbf{k}_2 are their quasimomenta, and $\mathbf{Q} \approx 0$ is the wave vector of the light. Taking the conservation laws (8.10) into account we obtain from (8.6) a final expression for the absorption coefficients

$$\alpha(\nu) = C\nu^2 \left(\frac{dE(\mathbf{k})}{d\mathbf{k}} \right)^{-1} |S(\mathbf{k})|^2. \quad (8.8)$$

Thus, the shape of the two-magnon absorption band is determined by the spectral distribution of the density of states in the spin-wave band $(dE(\mathbf{k})/d\mathbf{k})^{-1}$ and by the dependence of the probability of simultaneous excitation of two ions on the wave vector of the magnon $S(\mathbf{k})$. The constant C depends on the concrete mechanism whereby the transitions are induced.

Knowing the spin-wave dispersion law for the concrete crystal, we can determine the density distribution of the magnon state. Figure 21 shows the critical points in the distribution of the state density for the case of MnF_2 . The exchange constants used in the calculations are $J_1 = 0.34^\circ\text{K}$, $J_2 = 1.74^\circ\text{K}$, and $J_3 = 0.05^\circ\text{K}$ between the first, second, and third neighbors, respectively, and the magnetic anisotropy field employed was $H_A = 1.05^\circ\text{K}$. In antiferromagnetic fluorides of the iron group, the selection rules are such that for an electric vector $\mathbf{E}_\omega \parallel C_4$ a singularity appears in the two-magnon absorption line shape at the point A of the Brillouin zone, while for $\mathbf{E}_\omega \perp C_4$ the corresponding singularity lies at the point X.

From relation (8.8) and the known spin-wave dispersion law we can determine the frequency of the absorption maximum:^[90]

$$2\nu_M = 2(\nu_A + \nu_E). \quad (8.9)$$

If $\mathbf{k} \parallel C_4$ axis; $\nu_A = \gamma H_A$ and $\nu_E = \gamma H_E$ (H_A and H_E are the anisotropy and exchange fields and γ is the gyromagnetic ratio) are connected with the antiferromagnetic resonance frequency by:

$$\nu_{AFMR} = (\nu_A^2 + 2\nu_A\nu_E)^{1/2}. \quad (8.10)$$

Using, for example for FeF_2 , the known values $\nu_{AFMR} = 53 \text{ cm}^{-1}$ and $\nu_A/\nu_E = 0.371$, we obtain for two-magnon absorption $2\nu_M = 154 \text{ cm}^{-1}$, in splendid agreement with the experimental value 154.4 cm^{-1} .^[86] On the other hand, for the quantitative theory of the shape of the observed two-magnon absorption, it is necessary to specify concretely the mechanism of simultaneous excitation of two magnetic ions. Halley and Silvera,^[86,91] proposed a "spin-orbit" mechanism of "pairing" of two ions, while Tanabe, Moriya, and Sugano (TMS),^[83,92] who verified the Halley and Silvera "exchange" mechanism on the basis of the Coulomb interactions between the ions, have shown the "pairing" between the ions can occur as a result of interaction between the electron dipole moment of the ion i and the electric quadrupole moment of the ion j . This interaction is induced by the spin-orbit interaction if a high-frequency spin wave with $\mathbf{k} \neq 0$ is excited. In this case the energies of the even exciton states of the magnetic ion appear in the denominators of the theoretical expressions for A, A*, and B

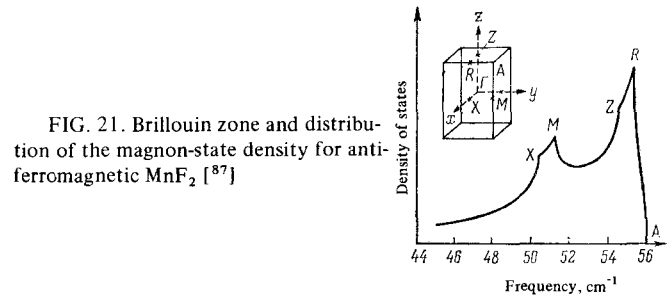


FIG. 21. Brillouin zone and distribution of the magnon-state density for antiferromagnetic MnF_2 [⁸⁷]

of the Hamiltonian (8.5) the i.e., a virtual allowed magnetic-dipole transition in the crystal, between the nearest even exciton states of the magnetic ion, occurs in the Halley-Silvera mechanism. It should be noted that the nearest even excited state for the Fe^{2+} ion is located $1000\text{--}2000 \text{ cm}^{-1}$ above the ground state, whereas for the Mn^{2+} ion this interval amounts to $\sim 20,000 \text{ cm}^{-1}$. In this connection, in accordance with the Halley-Silvera theory, the intensity of the two-magnon absorption in the case of MnF_2 should be smaller by four orders of magnitude than in the case of FeF_2 . Yet experimentally these quantities are of the same order.

This disparity, however, is eliminated when the TMS mechanism is used. The "pairing" between the two magnetic ions is then the result of superexchange interaction between them. A virtual electric dipole transition between two odd states of the magnetic ion, which goes beyond the limits of the 3d shell, and is allowed in the crystal, takes part in the process. Since the aforementioned odd excited states have comparable energies for the Fe^{2+} and Mn^{2+} ions, the intensity of the two-magnon absorption lines should be of the same order. According to the theory, the line in MnF_2 should be weaker by a factor of four than in FeF_2 , which agrees with the experimentally observed value ~ 2.5 .^[87] The foregoing considerations allow us to conclude that the Halley-Silvera theory is apparently not universal for all the iron-group metals. However, as shown by a comparison with the experimental results for FeF_2 , it can explain the main features of two-magnon absorption in the case of ions with appreciable spin-orbit interaction in the ground state. The Halley-Silvera mechanism explains the frequency of the absorption band in FeF_2 (154.4 cm^{-1}) and its temperature dependence and polarization, and qualitatively also the temperature dependence of the band intensity.^[86,91] As to the shape of the band, it follows from Fig. 22 that the theory gives a sharper "red" asymmetry with a distinct short-wave edge, whereas the experimentally observed shape is less asymmetrical. The authors of the theory have proposed that this is connected with neglect of the relaxation effects.

In the case of MnF_2 , satisfactory agreement with the experimental data concerning the shape of the band were obtained by Allen and co-workers^[87] on the basis of the TMS mechanism with allowance for the interaction between the magnetic ion and not only the nearest neighbors but also the more remote ones (Fig. 22a). Allowance for the nearest neighbors only gives a shape analogous to the case of FeF_2 .^[87] This apparently offers evidence that the real interaction range is longer than that of the exchange interaction. However, in the case of MnF_2 the short-wave edge of the band turned out to be

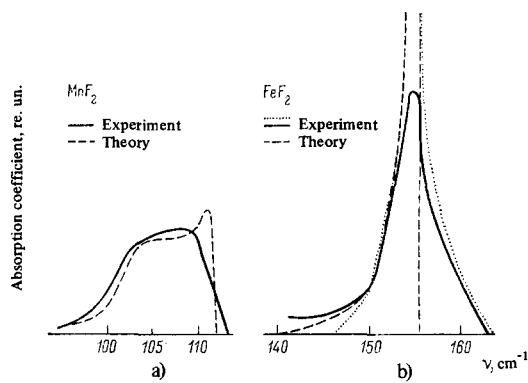


FIG. 22. Experimental two-magnon absorption line shape for MnF_2 (a) [87] and FeF_2 (b) [86]. Theoretical curves: a) TMS with allowance for long-range interaction; b) Halley-Silvera theory with allowance for interaction with the nearest neighbors. The two experimental curves in case b) correspond to different methods of separating the absorption background [86]. The intensity scales are different in (a) and (b).

sharper in the calculation than that observed experimentally.

The insensitivity of the experimentally observed band to the external magnetic field follows from the assumption that in the process under consideration the two magnons appear in opposite sublattices. In the TMS theory this naturally follows from the form of the superexchange interaction constant. In this case the external field increases the frequency of the magnon in one sublattice and decreases it in the other; consequently, the experimental band is independent of the field. Taking into account the qualitative difference between the experimental shapes of the bands of two-magnon absorption for the crystals MnF_2 and FeF_2 (Fig. 22) and the difficulties encountered by Allen and co-workers [87] in explaining the band shape in the case of MnF_2 , Halley proposed a third mechanism to explain two-magnon absorption in MnF_2 . [91] This mechanism is based on allowance for second-order mechanism and can be illustrated by Fig. 23. The electric field of the light wave interacts with the optical phonons of the crystal, which in turn interact with the spin waves via a magnetically-ordered interaction. The phonon that takes part in such a process is virtual. As shown by Halley, allowance for the indirect interaction between light and the spin waves leads to a Hamiltonian that includes the terms used by Allen et al. in the phenomenological interpretation of their results. With the aid of the developed theory it was possible to explain qualitatively the difference between the band shapes of MnF_2 and FeF_2 , as well as their weak dependence on the external field. However, no quantitative estimates were obtained, in view of the lack of information on the values of the constants of magnetically-ordered interaction, and also on the force constants and on the frequency of the optical phonons for MnF_2 .

The considered three mechanisms for the appearance of two-magnon absorption in antiferromagnetic fluorides explain the main experimental results in each concrete case. This gives grounds for assuming that they are competing mechanisms, and that each of them can prevail in a concrete case. None of the described mechanisms, however, explains the experimentally de-

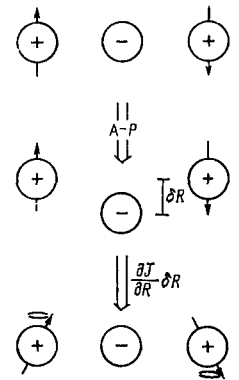


FIG. 23. Schematic illustration of the physical nature of Halley's "magnetically ordered" mechanism [91]. The initial, intermediate (virtual), and finite states of the system are shown in sequence.

veloped short-wave wing observed in the investigated absorption bands. This fact must be regarded as the main shortcoming of these mechanisms.

A thorough analysis of the shapes of two-magnon absorption bands may turn out to be very useful, since it can serve, in conjunction with information on the crystal symmetry, as a method of optically identifying the energies of the singular points on the boundary of the Brillouin zone. Even the average value of the magnon frequency on the boundary of the Brillouin zone is obtained from optical data much more readily than from investigations on neutron scattering.

b) **Phonon-magnon absorption.** In the infrared region of the absorption spectrum of the crystals Ni (1100 and 1940 cm^{-1}) [88-94] and KNiF_3 (1230 cm^{-1}) [95] there were observed bands which, like the previously considered two-magnon bands, are apparently connected with antiferromagnetic ordering. These bands depend strongly on the temperature. With increasing temperature, their maximum shifts towards longer wavelengths, and the spectral width of the lines increases in such a way that the band merges completely with the background near T_N .

A mechanism for explaining the observed absorption was proposed by Koide, Mizuno, and Tsuchida. [93] They have noted that in Ni and KNiF_3 crystals, where each pair of the magnetic ions has a symmetry center, the TMS mechanism cannot lead to the occurrence of magnon-induced electric-dipole transitions. In this connection, the lattice vibrations should play an important role in the explanation of the absorption bands that depend on the magnetic ordering. The observed bands were attributed to an electric-dipole transition, induced in a spin system by an optical phonon (see Sec. 3) and including the excitation of two magnons and one phonon. Using the Weiss approximation for the exchange interaction, the authors obtained the transition energy at $T \ll T_N$:

$$h\nu_S^{\pm} = 2h\nu_M \pm h\nu_K \quad (8.11)$$

where $h\nu_M = 2zJ \langle S_Z \rangle$ is the exchange-interaction energy and $h\nu_K$ is the phonon energy. The temperature dependence of $h\nu_S$ is obviously determined mainly by the analogous dependence for $\langle S_Z \rangle$. The theoretically obtained temperature dependences of the frequency and of the absorption band shape are in satisfactory agreement with the experimental results.

c) **Magnon satellite bands in the optical spectrum.** Insofar as we know, the first manifestation of additional light-absorption bands in the spectra of rare-earth iron garnets were observed by Krinchik and co-authors, [54-55]

Table I. Optical transitions for different antiferromagnetic crystals, in which exciton-magnon satellites were experimentally observed

Ion	Optical transition	Substance	Reference
Mn ²⁺	${}^6A_{1g}({}^6S) \rightarrow {}^4T_{1g}({}^4G)$	MnF ₂	50, 51, 82, 97, 98
	${}^6A_{1g}({}^6S) \rightarrow {}^4T_{1g}({}^4G)$	KMnF ₃	103
	${}^6A_{1g}({}^6S) \rightarrow {}^4T_{1g}({}^4G)$	RbMnF ₃	103
	${}^4T_{1g}({}^4G) \rightarrow {}^6A_{1g}({}^6S)$	MnF ₂	103
	${}^6A_{1g}({}^6S) \rightarrow {}^4A_{1g}({}^4F_g)$	MnF ₂	99, 100
	${}^6A_{1g}({}^6S) \rightarrow {}^4A_{1g}({}^4F_g)$	KMnF ₃	99, 100
	${}^6A_{1g}({}^6S) \rightarrow {}^4A_{1g}({}^4F_g)$	RbMnF ₃	103
	${}^6A_{1g}({}^6S) \rightarrow {}^4A_{1g}({}^4F_g)$	CsMnF ₃	103
	${}^6A_{1g}({}^6S) \rightarrow {}^4T_{2g}({}^4F)$	MnF ₂	103
	${}^6A_{1g}({}^6S) \rightarrow {}^4F_g({}^4D)$	MnF ₂	37
	${}^6A_{1g}({}^6S) \rightarrow {}^4F_g({}^4D)$	KMnF ₃	37
	${}^6A_{1g}({}^6S) \rightarrow {}^4F_g({}^4D)$	RbMnF ₃	101
	${}^6A_{1g}({}^6S) \rightarrow {}^4T_{1g}({}^4P)$	MnF ₂	82, 102
	Fe ²⁺	${}^5T_{2g} \rightarrow {}^3T_{2g}$	FeF ₂
${}^5T_{2g} \rightarrow {}^5E_g$		FeF ₂	21
Ni ²⁺	${}^3A_{2g} \rightarrow {}^1T_{2g}$	NiF ₂	60
	${}^3A_{2g} \rightarrow {}^1E_g$	KNiF ₃	82, 107
Co ²⁺	${}^4T_{1g}({}^4F) \rightarrow {}^4T_{2g}({}^4F)$	CoF ₂	

who also interpreted the additional bands as electron transitions accompanied by spin-wave production.

In Table I is gathered the most reliable information, in our opinion, concerning the additional absorption bands observed in the optical spectrum of antiferromagnetic crystals at $T < T_N$. A more detailed table is given in Sell's brief review.^[103] These bands are called magnon satellites or exciton-magnon transitions. It is characteristic that the magnon satellites are connected with electric-dipole transitions, are separated from the purely electronic transition by an interval $\sim kT_N$, are strongly polarized, and exist when $T < T_N$; some of them are characterized by a clearly pronounced "red" asymmetry, whereas others are practically symmetrical.

The first attempt to explain the additional "magnetic" bands was undertaken by Tanabe and Sugano.^[53] They noticed first of all that the appearance of additional lines cannot be attributed to simple splitting of the ground or excited level in the exchange field H_E . In addition to the usual electronic transitions in Ni²⁺, these authors considered also transitions in which one photon is absorbed by two exchange-coupled ions, one of which goes over to the excited state, and the other to the Zeeman component $m_S = 0$ of the ground state, which is split by the exchange field H_E ($\Delta m_S = +1$). In addition to such a double transition, ordinary single transitions are also possible. Such an analysis explains the appearance, following the magnetic ordering of the crystals, of satellites that are separated from the ground bands by an interval $\Delta\nu_M \sim g\mu_B H_G \approx kT_N$. However, it is impossible to explain within the framework of this theory the shapes of the additional bands and the temperature dependence of the band shape. To solve these problems it is necessary to take into account the collective character of the excitations (excitons, magnons) and the energy dispersion in the spin-wave band, whose width may be appreciable.^[51, 52]

It must be emphasized that the additional bands are connected with electric-dipole transitions, which are forbidden in the crystal (Sec. 3) if the ion is located at the symmetry center. In analogy with the mechanism described earlier (Sec. 3) for the appearance of phonon

satellites, the magnons can change the local symmetry, leading to the appearance of electric dipole magnon satellites. Such a process can be brought about by the mechanisms considered in Sec. 8a. In this case the Hamiltonian of the exciton-magnon electric-dipole transition can be obtained by summing in (8.2) over all pairs of ions in the crystal.

In Fig. 24, the exciton-magnon transitions are illustrated by diagrams from the paper of Halley and Silveira.^[84] The same figure shows the schemes of the exciton-magnon transitions, demonstrating the satisfaction of the energy and momentum conservation law (8.10) in such transitions. Figure 24 illustrates also the particular case of exciton-magnon transitions when two quasiparticles of the same kind, namely two magnons with equal but opposite momentum directions, are excited following the absorption of the photon.

Obviously, if we disregard the dispersion in the exciton band, which is negligibly small (Sec. 5), then the shape of the exciton-magnon band, as well as of the two-magnon bands, is determined by Eq. (8.8), and its max-

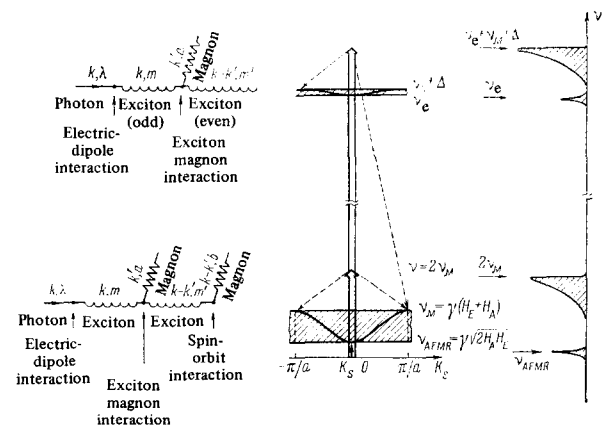


FIG. 24. Diagram and scheme illustrating the mechanism of exciton-magnon transitions in antiferromagnets: a) exciton-magnon transition; b) two-magnon transition. ν_{AFMR} - frequency of antiferromagnetic resonance; ν_M - frequency of spin waves with maximum momentum; ν_e - minimal exciton energy; Δ - width of exciton band ($\Delta \gg (\nu_M - \nu_{AFMR})$).

imum is shifted towards the short-wave side from the purely electronic line by an amount equal to the maximum energy of the spin waves ν_M (8.9).

The first to analyze the shape of the exciton-magnon band and to compare it with the structure of the optical absorption spectrum in the region of the longest-wavelength electronic transition ${}^6A_{1g}({}^6S) \rightarrow {}^4T_{1g}({}^4G)$ in manganese fluoride were Greene et al.^[50] The spectrum of this transition consists of two narrow weak magnetic dipole lines E1 (18419.6 cm^{-1}) and E2 (18436.6 cm^{-1}) and three broad relatively strong electric dipole lines σ_1 (18477.1 cm^{-1}), σ_2 (18485.3 cm^{-1}), and π_1 (18460.8 cm^{-1}). The magnetic dipole lines and the two σ lines are observed in σ polarization, while π_1 is observed in π polarization. The authors identified the E1 and E2 bands as exciton excitations, and the σ_1 band as a spin-wave satellite of the E1 band, which occurs upon simultaneous creation of an exciton and a magnon. Investigations by Russel, McClure, and Stout^[82] of the Zeeman effect and by Dietz and co-authors^[98] of the influence of the actual pressure on the behavior of this group of bands has made it possible to propose that σ_1 and π_1 are spin-wave satellites of E1, whereas σ_2 is a satellite of E2.

Greene and co-authors^[50] have shown that the shape of the electric-dipole absorption bands, their spectral position (they are separated from the purely electronic bands by $\Delta\nu = \nu_M + \Delta = 57 \text{ cm}^{-1}$, where $\nu_M = 55 \text{ cm}^{-1}$ is the maximum frequency of the spin waves and $\Delta = 2 \text{ cm}^{-1}$ is the width of the exciton band) agree with the assumed exciton-magnon mechanism of light absorption. The result of a comparison of the calculated and experimental investigations of the spectral distribution of the absorption coefficient in the region of the satellite band is shown in Fig. 25, which is taken from^[50]. The agreement is perfectly satisfactory if account is taken of the fact that no consideration was given to the finite lifetime in the excited state and to the nonzero value of temperature. A more detailed interpretation of the exciton-magnon bands of the ${}^6A_{1g}({}^6S) \rightarrow {}^4T_{1g}({}^4G)$ transition with allowance for magnetic symmetry of MnF_2 is given by a number of authors,^[51,52,102] who developed the TMS mechanism for this case. The polarization of the absorption bands has been explained. The experimentally observed difference in the shapes of the two-magnon absorption bands and of the magnon satellites of the ${}^6A_{1g}({}^6S) \rightarrow {}^4T_{1g}({}^4G)$ transition have been quantitatively demonstrated. The latter is clear from a comparison of the experimental curves of Figs. 22 and 25. This circumstance can be qualitatively understood by taking into account the fact that the appearance of the satellite bands in the optical spectrum and of the two-magnon absorption bands in the far infrared region is connected with the excitation of spin waves in different singular points of the Brillouin zone. As noted earlier (Sec. 8a), the π and σ two-magnon bands in MnF_2 are connected with excitation of spin waves with \mathbf{k} -vectors at the points A and X of the Brillouin zone respectively (see Fig. 21). The satellite π_1 in the optical spectrum has a shape which is not similar to σ absorption in the infrared spectrum. The shape of σ_1 demonstrates that it is the result of excitation of spin waves with $\mathbf{k} \parallel C_4$ - tetragonal axis at the point Z of the Brillouin zone. The energies of the spin waves with \mathbf{k} vectors at the points A and Z of the zone are approximately equal, and the

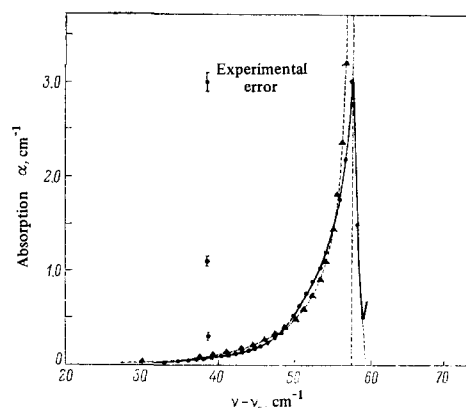


FIG. 25. Spectral distribution of the light-absorption coefficient in the region of the exciton-magnon absorption band ($T = 2.2^\circ\text{K}$)^[50].

● — calculation in accordance with (8.2); ▲ — experiment.

energy difference between A and X is of the order of 5 cm^{-1} . At the same time, the experimental difference between the π_1 and σ_1 peaks is 16 cm^{-1} . Tanabe and Gondaira^[102] could not explain this difference within the framework of the theory developed by them, even when account was taken of the width of the exciton band ($\Delta \sim 3 \text{ cm}^{-1}$). Nor was it possible to explain the singularities of the shapes of the σ_2 and π_1 bands, which reveal no clearly pronounced "red" asymmetry, or the fact that the π_2 band was not observed experimentally. These questions, and also details of the behavior of the satellites of the ${}^6A_{1g}({}^6S) \rightarrow {}^4T_{1g}({}^4G)$ transition of MnF_2 under pressure,^[98] remain unclear to this day and call for additional investigations. The exciton-magnon bands in the region of the ${}^6A_{1g}({}^6S) \rightarrow {}^4T_{1g}({}^4G)$ transition of the absorption spectrum of MnF_2 were investigated in greatest detail both experimentally and theoretically. This is connected with the fact that the ground state of the Mn^{2+} ion ($3d^5$ configuration) is ${}^6A_{1g}$, and the spin-wave spectrum is the simplest one, since there is no spin-orbit interaction. On the other hand, for the remaining ions of the iron group (Fe^{2+} , Co^{2+} , and Ni^{2+}) the situation is more complicated. For example, the ground state of the Fe^{2+} ion is the result of the ${}^5T_{2g}$ state, near which there are several exciton states. The transition to one of them, 5E_g , leads to an intense spin-allowed exciton transition, for which a magnetic dipole satellite is observed.^[104] It is possible that in the case of FeF_2 an important role may be played by the spin-orbit interaction proposed by Halley and Silvera.^[86] For the Ni^{2+} ion, we have investigated in greater detail^[21] the section of the spectrum corresponding to the ${}^3A_2 \rightarrow {}^1T_2$ transition in NiF_2 (see Fig. 6). Besides the exciton-magnon band $\nu = 20621 \text{ cm}^{-1}$, a two-magnon band, corresponding to a transition including two magnons (ν_M) and an exciton (ν_{∞}) was observed in the spectrum. This peak is located accordingly at a distance $2\nu_M$ from the purely electronic transition. A similar result was obtained by Van der Ziel and Guggenheim,^[107] who observed in compounds containing the Co^{2+} ion two-exciton transitions corresponding to the case when the final excited states of both ions of the pair correspond to exciton states.

Particular interest attaches to exciton-magnon transitions in the spectrum of the cubic antiferromagnet

RbMnF_3 .^[100] The period of the magnetic structure of this crystal is equal to double the period of the crystal structure ($a_M = 2a_K$). Taking this circumstance into account, it is easy to show that the "pairing" parameter S_m is equal to zero in the expression for the absorption coefficient (8.8) on the edge of the Brillouin zone ($k = \pi/a$) and is maximal on the edge of the magnetic Brillouin zone ($k = \pi/2a$).^[50] It follows therefore that in the optical spectrum there should appear predominantly spin waves with energy $E(\pi/2a)$ and not $E(\pi/a)$. According to neutron-diffraction data, $E(\pi/a) = 72 \text{ cm}^{-1}$ and $E(\pi/2a) = 56 \text{ cm}^{-1}$. The intervals $\Delta\nu = 56 \text{ cm}^{-1}$ is clearly separated in the optical spectrum.^[99,100] This equality agrees well with the assumption that the satellite bands in RbMnF_3 have an exciton-magnon nature, all the more since their shape and the temperature dependence of the spectral position also confirm this hypothesis.

Just as in the case of tetragonal fluorides (MnF_2 and NiF_2), exciton-magnon transitions in the cubic antiferromagnetic RbMnF_3 , judging from the intensities, are electric-dipole. But the magnonless bands in the spectra of the tetragonal fluorides are due to weak magnetic-dipole transitions, and in RbMnF_3 they are no less intense than the electron-magnon satellites. This suggests that the magnonless bands are in themselves already combined (electron-phonon) bands, and the satellite bands are due to transitions in which an exciton, phonon, and a magnon are simultaneously produced.

Such complicated optical transitions are realized also in tetragonal antiferromagnets, for example MnF_2 . This statement is based above all on an analysis of the behavior of the magnetic satellites in an external field. It was noted above that in spite of the collective exciton character the magnetic dipole purely electronic absorption lines are split^[82] in an external magnetic field $H \parallel C_4$, since the electronic excitation migrates over the ions of "only one sublattice,"^[51] and the external fields lift the "sublattice degeneracy." The electron-vibrational (electric-dipole) bands in an external electric field H oriented along the C_4 axis and having a lower intensity than H_C do not become split. Apparently, this is not surprising, since the field $H \parallel C_4$ does not change the magnetic symmetry of the crystal, and the interaction with oscillations that are asymmetrical relative to the inversion center "mixes" the electronic excitations of both sublattices, so that there is no "sublattice" degeneracy for such states. Since the spin-wave branch of the spectrum splits in a field $H \parallel C_4$ into two, this explains the behavior of the magnon satellites of the magnetic-dipole and electric-dipole bands. To this end it is necessary to use an expression that determines the shape and the spectral position of the exciton-magnon band in the optical spectrum of the antiferromagnet, (8.8), and the expression for the spectrum of spin waves in a field $H_Z < H_C = \sqrt{2HAHE}$ and $H_Z > H_C$.^[101] The results of such a calculation are illustrated in Fig. 26. The bands of the "double" (exciton-magnon) transitions—satellites of magnetic dipole lines—should not split in an external field, since the Zeeman splitting of a purely electronic transition is compensated by the splitting of the spin-wave branch (see the lower part of Fig. 26); the doublet structure of the band at $H < H_C$ is due to more subtle features of the exciton-magnon interaction.^[50]

On the other hand, the electron-phonon-magnon tran-

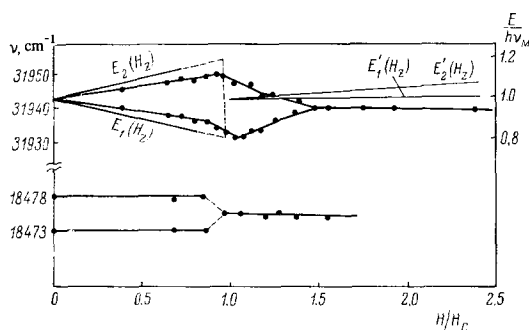


FIG. 26. Calculated and measured influences of the magnetic field on the light-absorption band in antiferromagnetic MnF_2 ($\nu_M = 55 \text{ cm}^{-1}$, $H_C \sim 9 \times 10^4 \text{ Oe}$)^[101].

sition bands (the magnon satellites of the electric-dipole bands) should be split in an external field, and this splitting is an unambiguous reflection of the behavior of the spin-wave branch of the spectrum (upper part of Fig. 26), since the electron-phonon band itself does not respond to the turning of a field $H < H_C$. The latter is connected with the fact that the electron-vibrational excitations due to the electric-dipole absorption apparently migrate over the ions of both sublattices. In this connection, the assumption^[50] that all the bands observed by us in the region of the ${}^6A_{1g}({}^6S) \rightarrow {}^4T_{2g}({}^4D)$ transition of MnF_2 ,^[80] which did not split in a field weaker than critical, are exciton-magnon bands can hardly be regarded as justified, especially if account is taken of the fact that almost all of them are observed in the paramagnetic phase of MnF_2 ($T > T_N = 68^\circ\text{K}$).

It follows from all the foregoing that the appearance of exciton-magnon absorption bands is usual in spectra of transition-metal ions in antiferromagnetic dielectrics. An investigation of the exciton-magnon absorption bands can yield valuable information concerning the excitons and magnons near the band boundaries, information difficult to obtain by other methods. More detailed investigations will make it possible to evaluate the dispersion of the exciton band, the energies of the singular points on the boundary of the Brillouin zone, the temperature dependence of the magnon energy, and the nature of the pair interaction. In spite of the fact that the main properties of the exciton-magnon bands are understood, some difficulties connected with their interpretation still exist and were mentioned earlier. In all the theoretical papers it is assumed that the exciton-magnon interaction is too small to change the dispersion law for excitons and magnons. This statement, however, calls for proof. In addition, it is necessary to take into account the influence of the phonons. Nor is the nature of the pair interaction completely clear. Therefore it is impossible to predict at present the relative intensity of the exciton-magnon bands for different exciton states in a given crystal. These theoretical problems cannot be solved, however, without additional reliable experimental information.

9. Influence of Electron-magnon Interaction on Magnonless Absorption Bands

The electron-magnon interaction is not only manifest by electron-vibrational satellites in the absorption spec-

trum, but also leads to a broadening of the phononless line. In magnetically-ordered crystals, similar effects are the result of interaction between the electrons of the absorbing center and the spin waves. In the preceding section we have dealt with the influence of electron-magnon interaction on the structure of the spectrum. Let us discuss now its influence on the shape and spectral positions of the magnonless absorption bands.

When investigating the shapes of magnonless light-absorption bands in MnF_2 crystals, we observed an anomaly of the temperature dependence of their width, [48] namely, the linear variation above the Neel temperature gives way to a much steeper dependence on going over to the antiferromagnetic state (Fig. 27). Similar singularities in the temperature dependence of the band widths were observed later for a number of other antiferromagnetic compounds (CoF_2 , [13-16] $CoCO_3$, [29, 46] and $CoCl_2$, [29] $MnCO_3$ [47, 49]). The observed anomaly offered unique evidence of the decisive role of the electron-magnon interaction in the formation of the contours of the absorption bands of antiferromagnetic crystals and stimulated the appearance of theoretical investigations of this question. V. A. Popov [108-110] considered the influence of spin waves on the shape of exciton (magnonless) absorption bands (see also, [110] while M. A. Krivoglaz and G. F. Levenson [11, 112] constructed a theory for the band shape of light absorption by local centers in magnetically ordered crystals. The results of the theoretical papers reduce qualitatively to the fact that the temperature dependence of the width and frequency of the optical band (in the region $T \ll T_N$) can be described by a power-law function, whose exponent ranges from 5/3 to 4, depending on the force of the electron-magnon interaction and on the character of the ordering (ferromagnetic or antiferromagnetic).

To verify the results of the theory, an experimental investigation was undertaken of the temperature dependence of the spectral position and the width of the nar-

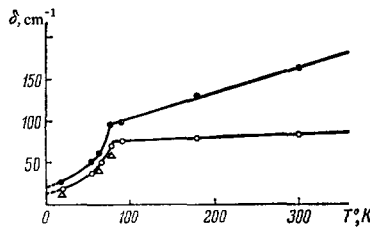


FIG. 27. Temperature dependence of the half-width of the C and D absorption bands of MnF_2 [48]. ● - C band, $E_\omega \perp C$ (σ component); ○ - C band, $E_\omega \parallel C$ (π component); Δ - D band, $E_\omega \perp C$.

row absorption bands in spectra of nickel compounds with different magnetic structures (NiF_2 , $RbNiF_3$, and K_2NiF_4). [113] Figures 28 and 29 show the temperature dependences of the shift $\Delta\nu = \nu_T - \nu_0$ and of the broad-

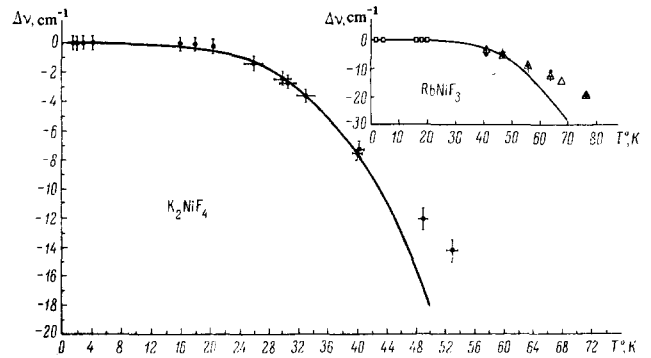


FIG. 28. Temperature dependence of the frequency shift of the maxima of the absorption bands in $RbNiF_3$ and K_2NiF_4 [113]. For $RbNiF_3$: ● - $\nu_0 = 20459 \text{ cm}^{-1}$, + - $\nu_0 = 20485.5 \text{ cm}^{-1}$, Δ - $\nu_0 = 22521 \text{ cm}^{-1}$; for K_2NiF_4 : $\nu_0 = 23579.2 \text{ cm}^{-1}$, $\Delta\nu = \nu_T - \nu_0$ (ν_T and ν_0 are the frequencies of the band at temperatures $T = 1.3$ and $20^\circ K$, respectively). In the interval $T = 1.3 - 20^\circ K$, there is no shift, and the points for all the bands of $RbNiF_3$ coincide at the given temperature and are designated by squares.

ening $\Delta\delta = \delta_T - \delta_0$ of several magnonless absorption bands. The frequencies of the bands were determined accurate to $\pm 0.2 \text{ cm}^{-1}$, and the error in the determination of the half width is $\pm 0.6 \text{ cm}^{-1}$. In the entire investigated temperature region, both the shift and the change of the half width for all the bands of one crystal are described by the same relationships (see Figs. 28 and 29), which can be represented by formulas [110]

$$\nu_T = \nu_0 + aT^l, \tag{9.1}$$

$$\delta_T = \delta_0 + bT^n. \tag{9.2}$$

A comparison of the experimental data, which could be carried out most thoroughly for the case of K_2NiF_4 (see Fig. 28), has shown that the shift of all the investigated magnonless absorption bands in the low-temperature region $T \leq 40^\circ K$ is proportional to T^4 ($l = 4$ in formula (9.1), the coefficient a varied from crystal to crystal). In Fig. 28, the solid curves were calculated theoretically in accordance with formula (9.1) with $l = 4$. The values of the coefficients a for the investigated bands are listed in Table II. With increasing temperature, the change becomes smoother and can be assumed to be proportional to $T^{5/2}$ or T^3 within the limits of experi-

Table II. Characteristic of the investigated optical bands in crystals containing Ni^{2+} [113]

Compound	Transition	$\nu_0, \text{ cm}^{-1}$	$\delta_0, \text{ cm}^{-1}$	$10^{-6} a, \text{ cm}^{-1}/\text{deg}^4$	$10^{-6} b, \text{ cm}^{-1}/\text{deg}^4$
$RbNiF_3$	$^3A_{2g} \rightarrow ^1T_{2g}^a$	20 458.4	10	1.2	1.7
	$^3A_{2g} \rightarrow ^1T_{2g}^b$	20 485.5	12.5	1.2	1.7
	$^3A_{2g} \rightarrow ^3T_{1g}^b$	22 521	25	1.2	1.7
K_2NiF_4	$^3A_{2g} \rightarrow ^3T_{1g}^b$	23 579.2	15.5	2.9	4.1

$\nu_0 - \delta_0$ - frequency and half-width of the band.

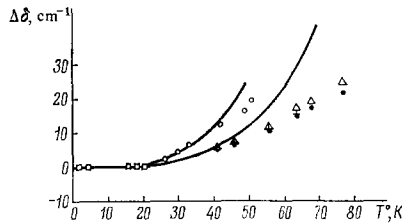


FIG. 29. Temperature dependence of the broadening $\Delta\delta = \delta_T - \delta_0$ of the absorption bands in RbNiF_3 and K_2NiF_4 [113]. For RbNiF_3 : \bullet — $\nu_0 = 20458.4 \text{ cm}^{-1}$, $+$ — $\nu_0 = 20485.5 \text{ cm}^{-1}$, Δ — $\nu_0 = 22521 \text{ cm}^{-1}$; for K_2NiF_4 : \circ — $\nu_0 = 23579.2 \text{ cm}^{-1}$ (δ_T and δ_0 are the half-widths at temperature $T = 1.3$ and 20°K , respectively). The bands do not broaden in the interval $T = 1.3 - 20^\circ\text{K}$, and the points for all the bands coincide at the given temperature and are designated by squares. Solid curves — theoretical calculations in accordance with formula (9.2) at $n = 4$.

mental error. The result obtained for $T \leq 40^\circ\text{K}$ agrees with the theoretical conclusions obtained by Popov (see [109, 110]). Within the framework of the model proposed by him, the broadening of the band is the result of interaction between the exciton and the magnons via the so-called “exchange spin-orbit interaction,” i.e., orbital excitation of an ion absorbing the light (exciton) is dissipated in spin excitations of the neighboring ions, due to the exchange interaction with the excited ion. Naturally, the band broadening due to this mechanism should depend on the exchange-interaction constant Θ_N . The constant a in formula (9.1) has an exchange character: [109]

$$\nu_T - \nu_0 = aT^4 = M(T_N) \left(\frac{T}{T_N}\right)^4, \quad (9.3)$$

where $M(T_N) = aT_N^4 = 7330 \text{ cm}^{-1} = 0.9 \text{ eV}$ for K_2NiF_4 . In this approximation [109]

$$M(T_N) \approx \frac{T_N^4}{\Theta_N^3} \approx T_N \left(\frac{T_N}{\Theta_N}\right)^3, \quad (9.4)$$

and therefore the exchange constant is $\Theta_N \sim 5.5 \times 10^{-3} \text{ eV}$, which coincides in order of magnitude with the estimate calculations of the exchange integral. [114]

Measurements of the band broadening are subject to large errors, so that at low temperatures it is more difficult to determine uniquely the exponent in formula (9.2). It can be stated that N lies in the range from $5/2$ to 4 . However, the linear relation between the shift and broadening in the entire investigated temperature region, for all the magnonless absorption bands, [113] gives grounds for assuming that the shift and broadening are described by the same law ($l = n$). This experimental result also agrees with the conclusions of the theory. [110] Table II lists the coefficients a and b in formulas (9.1) and (9.2) for all the investigated bands with $l = n = 4$ in the temperature interval $1.3^\circ \leq T \leq 4.2^\circ\text{K}$. It should be noted that good agreement with the theory cannot be expected in the entire temperature region, since the theory has been developed, strictly speaking, only for low temperatures ($T \leq 0.1T_N$), where the spin-wave approximation is valid. However, the obtained agreement between the experimental results and the conclusions of the theory can be regarded as proof of the correctness of the hypothesis that the “exchange spin-orbit” interaction mechanism considered by Popov determines the real broadening of the bands.

III. CONCLUSION

In this review we have considered only the singularities of light absorption in antiferromagnetic dielectrics. In a wide range of investigations of the interaction between light and magnetically-ordered crystals, the questions touched upon here have been investigated in greatest detail from the experimental point of view, and their theoretical interpretation is closest to completion. Although certain details of the light absorption mechanism in magnetically ordered crystals are not yet fully understood, this mechanism can already be regarded as a well corroborated method for investigating the structure of exciton and spin-wave bands.

Very closely related to the questions discussed above are investigations of absorption in the far infrared region—both resonant absorption, causing excitation of the lowest-frequency spin waves with zero quasimomentum (antiferromagnetic resonance), and nonresonant two-magnon absorption, which causes simultaneous excitation of two spin waves with maximum frequency and quasimomentum, corresponding to the boundary of the Brillouin zone. Such investigations have already yielded unambiguous information concerning the extremal values of the energy in the spin-wave spectrum of a number of antiferromagnetic crystals. Similar information is obtained from a study of Raman scattering of light by spin waves in antiferromagnets, observed in MnF_2 and FeF_2 , [115, 116] and theoretically explained in [117, 118]. A number of recent theoretical papers are devoted to investigations of Brillouin scattering of light by spin waves, [119, 120, 58] but this has not yet been observed experimentally.

We have not touched upon at all questions connected with singularities of luminescence and the Faraday effect in magnetically ordered crystals, which recently have been intensely investigated both in our country and abroad. Of course, without a detailed analysis of these secondary phenomena (Faraday effect, luminescence and scattering of light) it is impossible to obtain a complete representation of the interaction between light and magnetically ordered crystals. But such an analysis must be preceded by a discussion of the results of an investigation of the primary process, namely light absorption in magnetically ordered crystals, which we attempted to do in the present article.

¹ V. P. Babenko, V. L. Broude, V. S. Medvedev, and A. F. Prikhot'ko, *PTÉ* 1, 115 (1959).

² V. N. Pavlov and V. V. Eremenko, *PTÉ* 3, 208 (1967).

³ B. P. Zakharchenya and A. A. Sibilev, *Opt. Spektrosk.* 12, 616 (1962).

⁴ V. V. Eremenko and Yu. A. Popkov, *Ukr. Fiz. Zh.* 8, 88 (1963).

⁵ K. Aoyogi, A. Misy, and S. Sugano, *J. Phys. Soc. Japan* 18, 1448 (1963).

⁶ P. L. Kapitza, P. G. Strelkov, and É. Ya. Lauérman, *Zh. Eksp. Teor. Fiz.* 8, 276 (1938).

⁷ E. S. Borovik and A. G. Limar', *Zh. Tekh. Fiz.* 31, 939 (1961) [*Sov. Phys.-Tech. Phys.* 6, 683 (1961/62)].

⁸ H. A. Bethe, *Ann. d. Phys.* 3, 133 (1929); *Zs. Phys.* 60, 218 (1930).

⁹ C. J. Ballhausen, *Introduction to Ligand Field Theory*, McGraw-Hill, 1962.

- ¹⁰ L. Orgel, *Introduction to Transition-metal Chemistry*, Wiley, 1966.
- ¹¹ J. W. Stout and S. Reed, *J. Am. Chem. Soc.* **76**, 527 (1954).
- ¹² J. S. Griffith, *The Theory of Transition Metal Ions*, Cambridge Univ. Press, London, 1961.
- ¹³ H. Kamimura and Y. Tanabe, *J. Appl. Phys.* **34** (2), 1239 (1963).
- ¹⁴ A. I. Zvyagin, Dissertation, FTINT AN USSR (Low-temperature Institute) Khar'kov, 1966.
- ¹⁵ R. Newman and R. M. Chrenko, *Phys. Rev.* **115**, 1147 (1959).
- ¹⁶ A. I. Zvyagin and V. V. Eremenko, *Ukr. Fiz. Zh.* **10**, 526, 636 (1965).
- ¹⁷ V. I. Peresada and E. S. Syrkin, *Tr. Fiz.-tekh. in-ta nizkikh temperatur AN USSR*, No. 2, 335 (1968).
- ¹⁸ J. P. van der Ziel and H. J. Guggenheim, *Bell Telephone Laboratories*, New Jersey, Preprint.
- ¹⁹ R. Pappalardo, *J. Chem. Phys.* **31**, 1050 (1959).
- ²⁰ V. V. Eremenko, Doctoral Dissertation, FTINT AN USSR, Khar'kov, 1966.
- ²¹ A. I. Belyaeva, V. V. Eremenko, N. N. Mikhaïlov, V. N. Pavlov, and S. V. Petrov, *Zh. Eksp. Teor. Fiz.* **50**, 1472 (1966) [*Sov. Phys.-JETP* **23**, 979 (1966)].
- ²² M. Balkanski, P. Moch, and G. Pariset, *Compt. rend.* **258**, 2785 (1964).
- ²³ M. B. Balkanski, P. Moch, and M. K. Teng, *J. Chem. Phys.* **46**, 1621 (1967).
- ²⁴ V. V. Eremenko and A. I. Belyaeva, *Fiz. Tverd. Tela* **6**, 2877 (1963) [*Sov. Phys.-Solid State* **5**, 2106 (1964)].
- ²⁵ H. A. Bethe, *Intermediate Quantum Mechanics*, Benjamin, 1964.
- ²⁶ J. H. van Vleck, *Theory of Electric and Magnetic Susceptibilities*, Oxford University Press, London, 1932.
- ²⁷ A. D. Liehr and C. J. Ballhausen, *Phys. Rev.* **106**, 1161 (1957).
- ²⁸ V. V. Eremenko and A. I. Zvyagin, *Fiz. Tverd. Tela* **6**, 1013 (1964) [*Sov. Phys.-Solid State* **6**, 782 (1964)].
- ²⁹ A. I. Zvyagin, V. V. Eremenko, and I. V. Skorobogatova, *Ukr. Fiz. Zh.* **11**, 520 (1966).
- ³⁰ J. R. Ferraro and A. Walker, *J. Chem. Phys.* **42**, 1278 (1965).
- ³¹ D. S. McClure, *J. Chem. Phys.* **39**, 2850 (1963).
- ³² J. Ferguson, H. J. Guggenheim, and Y. Tanabe, *J. Appl. Phys.* **36**, 1046 (1965).
- ³³ W. H. Brumage, Ch. R. Yarger, and Ch. C. Lin, *J. Appl. Phys.* **35**, 994 (1964).
- ³⁴ W. H. Brumage, Ch. R. Yarger, and Ch. C. Lin, *Phys. Rev.* **133**, A765 (1964).
- ³⁵ J. Ferguson, H. J. Guggenheim, and Y. Tanabe, *Phys. Rev. Lett.* **14**, 737 (1965).
- ³⁶ J. Ferguson, H. J. Guggenheim, and Y. Tanabe, *J. Chem. Phys.* **45**, 1134 (1966).
- ³⁷ J. Ferguson, H. J. Guggenheim, and Y. Tanabe, *J. Phys. Soc. Japan* **21**, 692 (1966).
- ³⁸ B. S. Tsukerblat and Yu. E. Perlin, *Fiz. Tverd. Tela* **7**, 3278 (1965) [*Sov. Phys.-Solid State* **7**, 2647 (1966)].
- ³⁹ J. P. van der Ziel, *Phys. Rev. Lett.* **18**, 237 (1967); *Phys. Rev.* **161**, 483 (1967).
- ⁴⁰ V. V. Eremenko, V. N. Novikov, and Yu. A. Popkov, *Zh. Eksp. Teor. Fiz.* **54**, 1037 (1968) [*Sov. Phys.-JETP* **27**, 553 (1968)].
- ⁴¹ P. H. Cole and W. J. Ince, *Phys. Rev.* **150**, 377 (1966).
- ⁴² Y. Toyozawa, *Progr. Theor. Phys.* **20**, 53 (1958).
- ⁴³ A. S. Davydov and É. I. Rashba, *Ukr. Fiz. Zh.* **2**, 226 (1957).
- ⁴⁴ É. I. Rashba, *Izv. AN SSSR, ser. fiz.* **21**, 37 (1957).
- ⁴⁵ G. Elste, *Zs. Astrophys.* **33**, 39 (1957).
- ⁴⁶ V. V. Eremenko and A. I. Belyaeva, *Fiz. Tverd. Tela* **6**, 3646 (1964) [*Sov. Phys.-Solid State* **6**, 2918 (1965)].
- ⁴⁷ V. V. Eremenko and A. I. Belyaeva, *Fiz. Tverd. Tela* **6**, 1967 (1964) [*Sov. Phys.-Solid State* **6**, 1553 (1965)].
- ⁴⁸ A. I. Belyaeva and V. V. Eremenko, *Zh. Eksp. Teor. Fiz.* **44**, 469 (1963) [*Sov. Phys.-JETP* **17**, 319 (1963)].
- ⁴⁹ A. I. Belyaeva and V. V. Eremenko, *Zh. Eksp. Teor. Fiz.* **46**, 460 (1964) [*Sov. Phys.-JETP* **19**, 310 (1964)].
- ⁵⁰ R. L. Greene, D. D. Sell, W. H. Yen, A. L. Schawlow, and K. M. White, *Phys. Rev. Lett.* **15**, 656 (1965).
- ⁵¹ D. D. Sell, R. L. Greene, and K. M. White, *Phys. Rev.* **158**, 489 (1967).
- ⁵² R. Loudon, *Adv. Phys.* **17**, 243 (1968).
- ⁵³ S. Sugano and Y. Tanabe, Technical Report of Institute of Solid State Physics (ISSP) (Tokyo), ser. A, No. 71, (1963).
- ⁵⁴ G. S. Krinchik, *Fiz. Tverd. Tela* **5**, 373 (1963) [*Sov. Phys.-Solid State* **5**, 273 (1963)].
- ⁵⁵ G. S. Krinchik and G. K. Tyutneva, *Zh. Eksp. Teor. Fiz.* **46**, 435 (1964) [*Sov. Phys.-JETP* **19**, 292 (1964)].
- ⁵⁶ K. A. Wickersheim, *J. Appl. Phys.* **34**, 1224 (1963).
- ⁵⁷ K. H. Hellwege, S. Hüfner, M. Schinkmann, and H. Schmidt, *Phys. Lett.* **12**, 107 (1964); *Phys. Kondens. Materie* **4**, 108 (1965).
- ⁵⁸ I. A. Akhiezer and Yu. L. Bolotin, *Zh. Eksp. Teor. Fiz.* **53**, 267 (1967) [*Sov. Phys.-JETP* **26**, 179 (1968)].
- ⁵⁹ M. Balkanski, P. Mock, and R. G. Schulman, *J. Chem. Phys.* **40**, 1897 (1964).
- ⁶⁰ J. Knox, R. G. Schulman, and S. Sugano, *Phys. Rev.* **130**, 512 (1963).
- ⁶¹ R. V. Pisarev, *Fiz. Tverd. Tela* **7**, 1382 (1965) [*Sov. Phys.-Solid State* **7**, 1114 (1965)].
- ⁶² R. V. Pisarev, *Zh. Eksp. Teor. Fiz.* **49**, 1445 (1965) [*Sov. Phys.-JETP* **22**, 993 (1966)].
- ⁶³ R. V. Pisarev, *Fiz. Tverd. Tela* **8**, 2300 (1966) [*Sov. Phys.-Solid State* **8**, 1836 (1966/67)].
- ⁶⁴ N. N. Nesterova, I. G. Siniĭ, S. D. Prokhorova, and R. V. Pisarev, Paper of All-union Seminar on Magnetic Resonance and Spin Waves, Leningrad, 1967.
- ⁶⁵ J. Tsujikawa and E. Kanda, *J. phys. et radium* **20**, 352 (1959); *J. Phys. Soc. Japan* **18**, 1382 (1963).
- ⁶⁶ J. W. Stout, *J. Chem. Phys.* **31**, 709 (1959).
- ⁶⁷ D. M. Finlayson, J. S. Robertson, T. Smith, and R. W. H. Stevenson, *Proc. Phys. Soc.* **76**, 355 (1960).
- ⁶⁸ M. E. Lines, *Phys. Rev.* **A137**, 982 (1965).
- ⁶⁹ A. H. Cooke, K. A. Gehring, M. S. M. Leask, D. Smith, and J. H. M. Thornley, *Phys. Rev. Lett.* **14**, 685 (1965).
- ⁷⁰ A. I. Belyaeva, V. V. Eremenko, N. N. Mikhaïlov, and S. V. Petrov, *Zh. Eksp. Teor. Fiz.* **49**, 47 (1965) [*Sov. Phys.-JETP* **22**, 33 (1966)].

- ⁷¹ W. Holloway and M. Kestigian, *J. Appl. Phys.* **38**, 1480 (1967).
- ⁷² A. I. Zvyagin, V. V. Eremenko, and V. I. Kut'ko, *Fiz. Tverd. Tela* **7**, 3102 (1965) [*Sov. Phys.-Solid State* **7**, 2505 (1966)].
- ⁷³ K. A. Wickersheim, *Phys. Rev.* **122**, 1376 (1961).
- ⁷⁴ P. M. Levy, *Phys. Rev.* **135**, A155 (1964).
- ⁷⁵ G. F. Koster and H. Statz, *Paramagnetic Resonance*, vol. 1, Acad. Press, N.Y.-Lnd., 1963.
- ⁷⁶ G. S. Krinchik and M. V. Chetkin, *Zh. Eksp. Teor. Fiz.* **41**, 673 (1961) [*Sov. Phys.-JETP* **14**, 485 (1962)].
- ⁷⁷ A. I. Belyaeva, V. V. Eremenko, V. N. Pavlov, and A. V. Antonov, *Zh. Eksp. Teor. Fiz.* **53**, 1879 (1967) [*Sov. Phys.-JETP* **26**, 1069 (1968)].
- ⁷⁸ A. I. Belyaeva, V. N. Pavlov, and A. V. Antonov, *Fiz. Tverd. Tela* **10**, 683 (1968) [*Sov. Phys.-Solid State* **10**, 537 (1968)].
- ⁷⁹ C. V. Stager, *J. Appl. Phys.* **34**, 1232 (1964).
- ⁸⁰ V. V. Eremenko, Yu. A. Popkov, and Yu. G. Litvinenko, *Zh. Eksp. Teor. Fiz.* **47**, 1733 (1964) [*Sov. Phys.-JETP* **20**, 1165 (1965)].
- ⁸¹ V. V. Eremenko and Yu. A. Popkov, *Physica Status Solidi* **12**, 627 (1965).
- ⁸² P. G. Russel, S. D. McClure, and J. W. Stout, *Phys. Rev. Lett.* **16**, 176 (1966).
- ⁸³ T. Moriya, *J. Phys. Soc. Japan* **21**, 926 (1966).
- ⁸⁴ J. W. Halley and I. Silvera, *Phys. Rev. Lett.* **15**, 654 (1965).
- ⁸⁵ J. W. Halley and I. Silvera, *J. Appl. Phys.* **37**, 1226 (1966).
- ⁸⁶ I. Silvera and J. W. Halley, *Phys. Rev.* **149**, 415 (1966).
- ⁸⁷ S. J. Allen, R. Loudon, and R. L. Richards, *Phys. Rev. Lett.* **16**, 463 (1966).
- ⁸⁸ P. L. Richards, *J. Appl. Phys.* **38**, 1500 (1967).
- ⁸⁹ D. L. Dexter, *Phys. Rev.* **126**, 1962 (1962).
- ⁹⁰ C. Kittel, *Quantum Theory of Solids*, Wiley, 1963.
- ⁹¹ J. W. Halley, *Phys. Rev.* **154**, 423, 458 (1966).
- ⁹² Y. Tanabe, T. Moriya, and S. Sugano, *Phys. Rev. Lett.* **15**, 1023 (1965).
- ⁹³ R. W. Johnston and D. C. Cronmeyer, *Phys. Rev.* **93**, 634 (1954).
- ⁹⁴ R. Newman and R. M. Chrenko, *Phys. Rev.* **114**, 1507 (1959).
- ⁹⁵ A. Tsuchida, *J. Phys. Soc. Japan* **21**, 2497 (1966).
- ⁹⁶ S. Koide, Y. Mizuno, and A. Tsuchida, *Phys. Lett.* **13**, 8 (1964).
- ⁹⁷ D. D. Sell, R. L. Greene, W. M. Yen, A. L. Schawlow, and R. M. White, *J. Appl. Phys.* **37**, 1229 (1966).
- ⁹⁸ R. E. Dietz, A. Missetich, and H. J. Guggenheim, *Phys. Rev. Lett.* **16**, 841 (1966).
- ⁹⁹ A. V. Antonov, A. I. Belyaeva, and V. V. Eremenko, *Fiz. Tverd. Tela* **8**, 3397 (1966) [*Sov. Phys.-Solid State* **8**, 2718 (1967)].
- ¹⁰⁰ V. V. Eremenko, Yu. A. Popkov, V. N. Novikov, and A. I. Belyaeva, *Zh. Eksp. Teor. Fiz.* **52**, 454 (1967) [*Sov. Phys.-JETP* **25**, 297 (1967)].
- ¹⁰¹ V. V. Eremenko, Yu. A. Popkov, and L. T. Kharченко, *ZhETF Pis. Red.* **3**, 233 (1966) [*JETP Lett.* **3**, 149 (1966)].
- ¹⁰² Y. Tanabe and K. I. Gondaira, *J. Phys. Soc. Japan* **22**, 573 (1967).
- ¹⁰³ D. D. Sell, *J. Appl. Phys.* **39**, 1030 (1968).
- ¹⁰⁴ J. Tylicki and W. M. Yen, *Phys. Rev.* **166**, 488 (1968).
- ¹⁰⁵ T. Moriya and M. Inoue, Technical Report of ISSP, ser. A, No. 302, Tokyo, Japan, 1968.
- ¹⁰⁶ J. Tylicki, F. L. Scarpace, M. W. Passow, and W. M. Yen, *Bull. Am. Phys. Soc.* **12**, 285 (1967).
- ¹⁰⁷ J. P. van der Ziel and H. J. Guggenheim, *Phys. Rev.* **166**, 479 (1968).
- ¹⁰⁸ V. A. Popov, *Fiz. Tverd. Tela* **8**, 3339 (1966) [*Sov. Phys.-Solid State* **8**, 2666 (1967)].
- ¹⁰⁹ V. A. Popov, *Izv. AN SSSR, ser. fiz.* **20**, 927 (1966).
- ¹¹⁰ V. A. Popov and A. A. Loginov, *Trudy X Mezhdunarodnoi konferentsii po fizike nizkikh temperatur (Proc. Tenth Internat. Conf. on Low Temperature Physics)*, v. 4, Moscow, 1967.
- ¹¹¹ M. A. Krivoglaz and G. F. Levenson, *Fiz. Tverd. Tela* **9**, 457 (1967) [*Sov. Phys.-Solid State* **9**, 349 (1967)].
- ¹¹² M. A. Krivoglaz and G. F. Levenson, *Fiz. Tverd. Tela* **9**, 2693 (1967) [*Sov. Phys.-Solid State* **9**, 2114 (1968)].
- ¹¹³ A. I. Belyaeva and V. V. Eremenko, *Zh. Eksp. Teor. Fiz.* **54**, 1303 (1968) [*Sov. Phys.-JETP* **27**, 695 (1968)].
- ¹¹⁴ A. J. Freeman and R. E. Watson, *Phys. Rev.* **124**, 1439 (1961).
- ¹¹⁵ P. A. Fleury, S. P. S. Porto, and R. Loudon, *Phys. Rev. Lett.* **18**, 658 (1967).
- ¹¹⁶ P. A. Fleury, S. P. S. Porto, L. E. Cheesman, and H. J. Guggenheim, *Phys. Rev. Lett.* **17**, 84 (1966).
- ¹¹⁷ T. Moriya, *J. Phys. Soc. Japan* **23**, 490 (1967).
- ¹¹⁸ Y. R. Shen, *J. Appl. Phys.* **38**, 1490 (1967).
- ¹¹⁹ Y. R. Shen and N. B. Bloembergen, *Phys. Rev.* **143**, 372 (1966).
- ¹²⁰ V. S. L'vov, *Zh. Eksp. Teor. Fiz.* **53**, 163 (1967) [*Sov. Phys.-JETP* **26**, 113 (1968)].

Translated by J. G. Adashko